Optimization of Tensegrity Structures

by

Quentin Marzari

Diplôme d'ingénieur civil
École Nationale des Ponts et Chaussées, 2014

Submitted to the Department of Civil and Environmental Engineering in
Partial Fulfillment of the Requirements for the Degree of

Master of Engineering in Civil and Environmental Engineering

at the

Massachusetts Institute of Technology

June 2014

Signature redacted

Signature of Author: ________________

Department of Civil and Environmental Engineering
May 21, 2014

Certified by: ________________ Signature redacted

Pierre Ghisbain
Lecturer of Civil and Environmental Engineering
Thesis Supervisor

Certified by: ________________ Signature redacted ________

Jerome J. Connor
Professor of Civil and Environmental Engineering
Thesis Co-Supervisor

Certified by: ________________ Signature redacted ______

Heidi M. Nepf
Chair, Departmental Committee for Graduate Students

Optimization of Tensegrity Structures

by

Quentin Marzari

Submitted to the Department of Civil and Environmental Engineering on May 21, 2014
in Partial Fulfillment of the Requirements for the Degree of Master of Engineering in
Civil and Environmental Engineering

ABSTRACT

This thesis presents a new approach to solve the optimization of articulated structures and especially looks into the performance of tensegrity systems compared to regular trusses. Volume is the objective to minimize and a wide range of constraints can be considered from the required mechanical constraints to more architectural ones. The resulting nonlinear non-convex mixed-integer optimization problem is approached with a twofold algorithm. A global genetic algorithm controls the connectivity and geometric variables while the cross-sectional area and prestress forces variables are dealt with an internal sequential quadratic programming algorithm. The performance of this approach is evaluated on a typical cantilever configuration.

Keywords: Optimization, Tensegrity, Truss, Genetic Algorithm

Thesis Supervisor: Pierre Ghisbain
Title: Lecturer of Civil and Environmental Engineering

Thesis Co-Supervisor: Jerome J. Connor
Title: Professor of Civil and Environmental Engineering

Résumé

Cette thèse présente une nouvelle approche dans le cadre de l'optimisation des structures articulées. En particulier, la performance relative des systèmes de tenségrité par rapport à de simples treillis y est étudiée. Le volume est le critère d'optimisation et de nombreuses contraintes sont considérées allant des prérequis en terme de comportement mécanique jusqu'à des contraintes relevant plus de choix architecturaux. Le problème mathématique d'optimisation résultant est non convexe, non linéaire et mélange variables entières et continues. Sa résolution est abordée à l'aide d'un algorithme en deux parties. Un premier algorithme général, de type génétique, contrôle les variables associées à la géométrie et à la connectivité alors que, l'optimisation sur les variables correspondant à l'aire des éléments et à la précontrainte y résidant est prise en charge par un algorithme secondaire, de type quadratique séquentiel. La performance de cette méthode est évaluée sur un cas typique de poutre console.

Keywords : Optimisation, Tenségrité, Treillis, Algorithme génétique

Acknowledgments

First of all, I would like to thank my thesis advisors, Dr. Pierre Ghisbain and Prof. Maurizio Brocato, for the time they spent helping me on my research. Discussing with them was a real pleasure and I enjoyed confronting ideas with them.

Being a recipient of the Bourse Jacques Coiffard , I would like also to thank the members of the Fondation des Ponts for their support.

Table of Contents

Summary

Abstract 3

Résumé 5

Acknowledgments 7

Table of Contents 9

List of Tables 11

List of Figures 13

List of Appendices 15

Introduction 17

1. Motivations and introduction to tensegrity structures 19

  1.1 Motivations 19

  1.2 Tensegrity structures 21

    1.2.1 Definitions 21

    1.2.2 A few mechanical considerations 22

    1.2.3 Applications of tensegrity structures 25

  1.3 Literature review on the optimization of articulated structures 26

2. Formulation of the optimization problem 27

  2.1 Data and choice of the variables 27

    2.1.1 Geometry variables 28

    2.1.2 Connectivity variables 28

    2.1.3 Scale variables 29

    2.1.4 Note on the configurations 30

  2.2 Formulation of the optimization problem 30

    2.2.1 Objective function 30

    2.2.2 Constraints 31

    2.2.3 Important remarks on the formulation 35

    2.2.4 Summary 37

3. First examples 39
3.1 Truss optimization – No points added (n=0) 39
3.2 Tensegrity optimization – No points added (n=0) 42
3.3 Truss optimization – One added point (n=1) 44
3.4 Tensegrity optimization – One added point (n=1) 50
3.5 Specific derivation for isostatic systems 51
4. Computational approach to solve the general problem 55
4.1 Characteristics of the problem and approach 55
4.1.1 Choosing the starting points 55
4.1.2 Programming approach 56
4.2 Description of the algorithms 56
4.2.1 Genetic algorithm (GA) 56
4.2.2 Sequential Quadratic Programming (SQP) 57
4.3 Results 57
4.4 Remarks 60
Conclusion and perspectives 61
Bibliography 63
Appendices 67
Appendix 1 - Derivation of the static equilibrium equation with the stiffness method 69
A.1.1 Member stiffness matrix 69
A.1.2 Assembling the system stiffness matrix 69
A.1.3 Modification of the Static equilibrium equation to account for the supports 71
Appendix 2 - Determinant calculation 73

List of Tables

Table 1 Comparison of the design steps for truss and tensegrity 27
Table 2 Summary of the variables and expressions of the constraints and the objective function 38
Table 3 Results from the numerical optimization 59

List of Figures

Figure 1 : Cantilever situation 19

Figure 2 : Optimal cantilever frame according to Michell (Michell, 1904) 20

Figure 3 : Steel 3D printing at the *Joris Laarman* Lab in Amsterdam 21

Figure 4 : Two tensegrity systems – a) Snelson's X-piece (1948) and b) Bicycle wheel 22

Figure 5 : Mechanical Behavior of a) struts and b) cables from (Motro & Vassart, 2001) 22

Figure 6 : Different states of a soccer balloon from (Motro & Vassart, 2001) 23

Figure 7 : Different state of stress for a spring element 24

Figure 8 : Endothelial cells under the microscope (A) and tensegrity model (B) from (Ingber, 2003) 25

Figure 9 : Cantilever truss optimization (Jarre, Kocvara, & Zowe, 1998) 26

Figure 10 : Two configurations with one added point and different connectivities 28

Figure 11: Cantilever truss problem n=0 40

Figure 12: Surface plot of the volume function 41

Figure 13: Allowable member areas for α =360 42

Figure 14 : Allowable member areas for α =360 43

Figure 15 : Truss configuration n=1 44

Figure 16 : One potential optimal configuration for truss problem n=1 45

Figure 17 : Plan view of the minimum volume function $Vmin$ – Truss n=1 – member 2 removed 46

Figure 18 : 3D view of the minimum volume function $Vmin$ - Truss n=1 – member 2 removed 46

Figure 19 : Another potential optimal configuration for truss problem n=1 47

Figure 20 : Plan view of the minimum volume function $Vmin$ – Truss n=1 – member 4 removed 48

Figure 21 : 3D view of the minimum volume function $Vmin$– Truss n=1 – member 4 removed 48

Figure 22 : Plan view of the minimum volume function $Vmin$ – Truss n=1 – hyperstatic case . 49

Figure 23 : 3D view of the minimum volume function $Vmin$– Truss n=1 – hyperstatic case 49
Figure 24 : Evolution of the penalty value over the generations until convergence.................... 56

List of Appendices

Appendix 1 - Derivation of the static equilibrium equation with the stiffness method 69

Appendix 2 - Determinant calculation 73

Introduction

Optimization is a concept that surrounds us everywhere. In people's everyday decisions the question of the optimal choice is asked. In Nature as well, the optimization process is present. Shapes, materials, chemical reactions have been selected through many years of evolution. Nowadays, depending on the industry, the look for optimality is not the same. In Industrial Engineering, manufacturing processes will be studied and optimized as much as possible as it will increase profits. In Civil Engineering though, practitioners tend to pick standard solutions as a way to save money.

It is true that optimizing a quantity/price chart may be easier than trying to define a whole structure but, numerical optimization capabilities have significantly increased over the last decades. This thesis is an attempt to challenge this status quo and try to see how today's computational capabilities can solve a complex structural optimization problem.

The structural engineering problem chosen is the minimization of the mass of articulated structures. Both trusses and tensegrity systems, which is a specific type of articulated structures, are considered.

This document is composed of four parts. The first one presents the motivations for this research and introduces tensegrity structures. In the second part, the optimization problem is formulated in the typical framework of mathematical optimization. The third part is dedicated to present a few examples to apprehend the method and obtain first results. Finally, the last part presents the computational approach. Some results obtain numerically are displayed and discussed.

1. Motivations and introduction to tensegrity structures

1.1 Motivations

One of the teachers[1] I had at MIT always uses the same slide for the introduction lecture of his class on Structural Systems. It is a typical cantilever situation where a load is applied at a certain distance from a wall. His argument is that Structural Engineering is not reduced to the sizing of elements (for instance a beam here) but involves deciding how to transfer the load in the first place and eventually making sure that the load path created is adequate. The problem is therefore threefold and a designer must provide: a system, geometry and the scale or sizing (pending a material has been chosen). Quite often there is a gap in practice between the geometry step and the sizing. The former would be decided by an architect following aesthetics and functionality criteria while the latter would be the structural engineer's role. In the end, one would pick a structural system out of the few we know so far, pick a typical (regular) geometry, and then size the system.

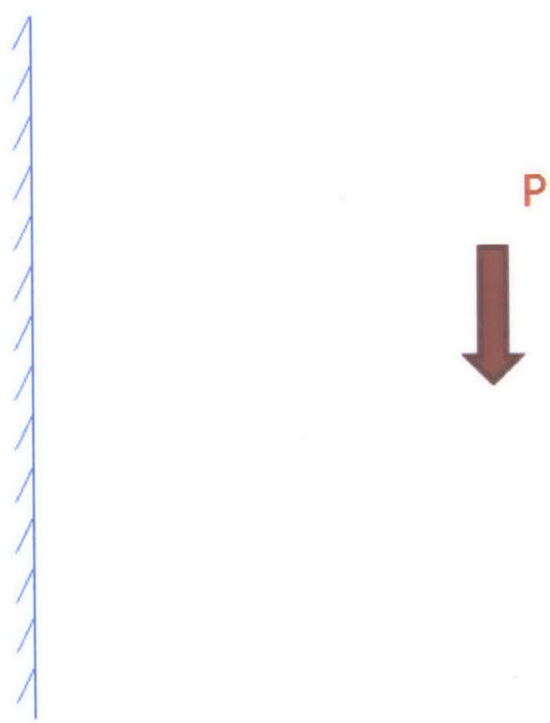

Figure 1 : Cantilever situation

In this example one would argue that a beam is required. If by beam, one means a system that can carry the bending moment which is generated by the support offset, then yes that is what is needed. Now, there are several ways of transferring moment from one point to another. One

[1] Mr. Paul Edward Kassabian teaching 1.572 Structural Systems at MIT

could be a solid beam, but another possibility could be a truss beam. Michell, showed the optimal configuration for a frame structure in a cantilever situation with two given maximum stresses (for the struts and ties) is one where all members have the same axial strain (Michell, 1904). Whatever the load value or the material chosen for the elements, the statement holds.

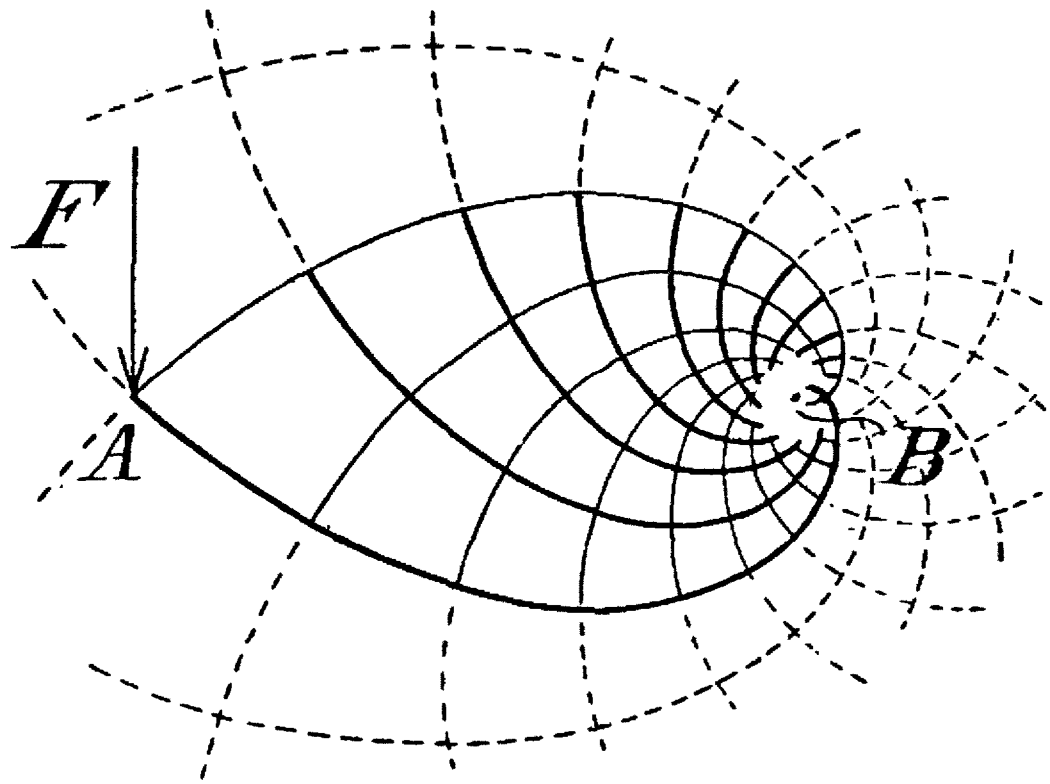

Figure 2 : Optimal cantilever frame according to Michell (Michell, 1904)

This reasoning is valid when only yielding constraints are considered. Indeed, for buckling constraints on compressive members, the relationship involves a critical force that varies with the inertia of the cross-section and the length of the member. In general, the inertia of an element is not a strictly increasing function of the area only. A solid rod is an exception as the inertia varies with the square of the area; however, this cross-section type is known not to be efficient material wise. Displacement constraints also have a complex expression. The stiffness of the whole structure, and thus the area of each member, is involved.

A rich literature exists about the study of optimal geometries for different problems and structural system. Some methods are heuristic like the determination of shells geometry by studying reduced scale models (a famous example is the *Sagrada Familia* by A. Gaudi). Various quantitative approaches have also been developed to find optimal geometries such that the term "form-finding" was introduced. In itself the problem is generally complex and the solution relies on numerical optimization capabilities.

Even if significant results exist, the lack of applications in the industry can be easily explained. In a market economy, having tune-shaped structural members is substantially more expensive than standardized elements for which construction methods are known and mastered. The

Construction sector is known for resisting innovation. Looking at the progress in 3D printing, one could argue that this current state might change soon. The Figure below shows a new method where a welding electrode is moved in space to 3D print with steel.

Figure 3 : Steel 3D printing at the *Joris Laarman* Lab in Amsterdam (http://techxplore.com/news/2014-02-3d-metal-amsterdam-lab-video.html)

In a modern perspective where the design of a structure is controlled by structural (strength and motion) and architectural requirements, my motivation in this text is to try optimizing a specific class of structure called "Tensegrity". The next section will introduce the matter.

1.2 Tensegrity structures

1.2.1 Definitions

The origin of Tensegrity systems goes back to the 1940s. The paternity is contested but it is safe to say that two of the first people to study and use them were Richard Buckminster Fuller and Keneth Snelson. The first one created the word from the contraction of the two words "tension" and "integrity" (Lalvani, 1996) while the second referred to them as "floating compression". A commonly accepted definition was proposed in 2003 by the scientific community. A tensegrity system is an articulated system in a state of stable prestress equilibrium composed of a discontinuous set of compression members (bars or struts) and a continuous set of tension members (cables or ties). In the canonical (regular) form, all the elements are rectilinear and the ones of the same type have the same length.

To increase the richness of this class of structure, I extend the tensegrity definition relaxing the regularity and continuity hypothesis on both struts and cables. This allows the formation of more complex assembly such as in Figure 4 a). In (Skelton & de Oliveira, 2009), they use an even broader definition where the compressive parts can have any geometry. This is a very fertile extension as a lot of common objects fall into the tensegrity framework such as a bicycle wheel where the spokes are the tension members and the wheel is the compressive part. For the rest of this document, I will focus on rectilinear compressive bodies (which can still be connected between each other). In a nutshell, a tensegrity system can then be viewed as a prestressed space truss where tension members are cables and compression members are struts. Often, they are classified depending on the maximum number of compressive elements joining at one node. The bicycle wheel will then be a "class 1" tensegrity system.

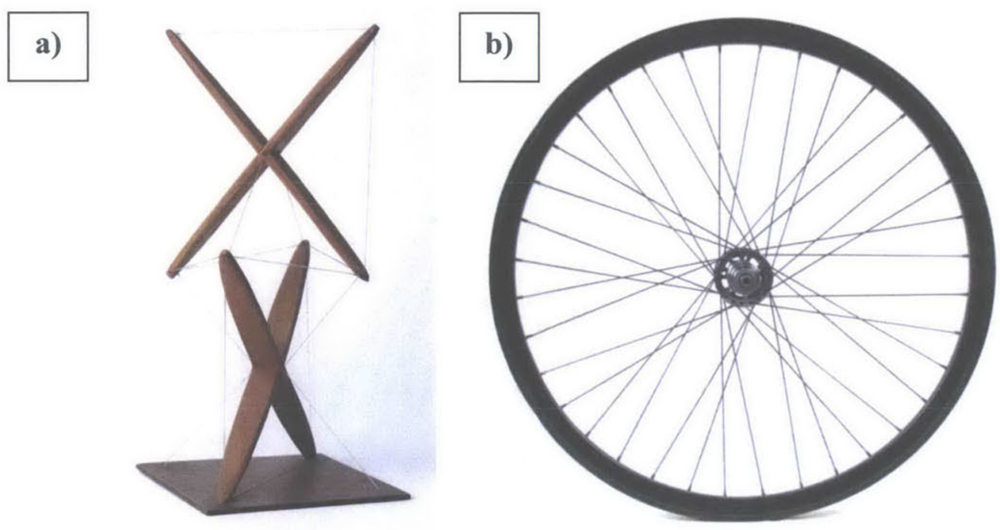

Figure 4 : Two tensegrity systems – a) Snelson's X-piece (1948) and b) Bicycle wheel

Another interesting feature that is worth mentioning is the dualisation. Every tensegrity system has a dual which is also a tensegrity system. The dual is obtained by inverting cables and bars in the configuration. Note that it may not be stable.

1.2.2 A few mechanical considerations

Several models can be considered for the behavior of the two types of element composing a tensegrity structure.

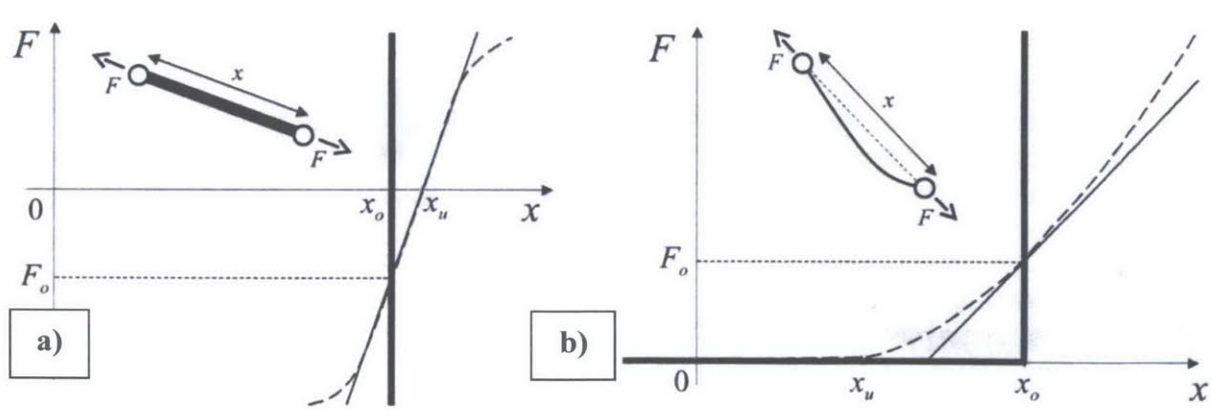

Figure 5 : Mechanical Behavior of a) struts and b) cables from (Motro & Vassart, 2001)

In the figure above, three behavior models for the members are represented. The bolded, full and dashed lines correspond respectively to the ideal infinitely rigid, the linearized, and the real behavior. Bars have a bilateral behavior while cables have a unilateral behavior. However, since cables are better in taking tension than bars, in the following we assume bars have a unilateral behavior that mirrors the cables'. Prestress in the system allows then some bilateral behavior for the two types of members. Pretensioned cables will then be able to take some compression; they will feel less tension than in the initial state.

It appears that steel cables have a significantly higher yielding limit while having a lower effective elastic modulus compared to a standard steel rod. Typical numbers given in (Latteur, 2006) are $E_c = 170GPa$ for a cable strand effective Young's modulus and $f_{y,c} = 1GPa$ for the yielding point. Hence, by having cables in a structure we increased its strength but lower its stiffness.

A counteracting effect to this loss of stiffness is the prestress in the tensegrity structure. Indeed, prestressing a structure increases its geometric rigidity while no alteration on the physical rigidity happened. To understand this, we can look at an analogy used in (Motro & Vassart, 2001).

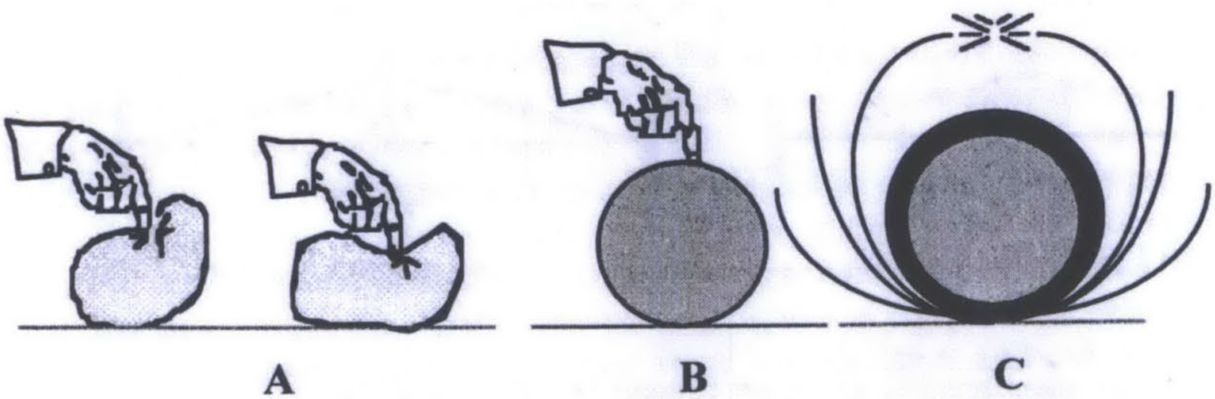

Figure 6 : Different states of a soccer balloon from (Motro & Vassart, 2001)

Let V be the volume of air inside the balloon and V_0 be the volume of the solid balloon envelope. We distinguish three cases:

- **A :** $V < V_0$, the balloon does not have a defined geometry. Depending on the loads applied to it the system "moves". It is kinematically indeterminate or statically unstable (hypostatic).

- **B :** $V = V_0$, the geometry is unique and the system is statically and kinematically determinate (isostatic). It can be referred to a null state of prestress.

- **C :** $V > V_0$, the pressure inside the balloon is higher than the atmospheric pressure. To enforce equilibrium the system expands. Tension is created in the envelope. The geometry is defined (slightly different than before). It is a statically indeterminate system (hyperstatic).

Comparing the apparent stiffness, it is clear that deforming the system by the same amount is more difficult in case C than B. The tradeoff, however, is a loss in the allowed stress range.

Similarly, a key parameter has been identified for regular tensegrity structures in (Motro & Vassart, 2001). The analogous of the volume V is the ratio $r = \frac{b}{c}$, where b is the length of the bars and c is the length of cables. A specific value r_0 (likeV_0), for which the system becomes kinematically determinate, can be identified.

Let's look now at a spring element of stiffness k and rest length l_0. Let us compare the case where the initial state corresponds to a null elongation, with the one where the initial state is offset by $l_1 - l_0$, i.e. the spring is prestressed. The associated prestress force is $F_0 = k(l_1 - l_0)$. Often, the stiffness of a spring is defined as the force required displacing the system of 1 unit of length from its rest position. Depending on the unit length chosen the value of the force obtained is the same as the value of the system stiffness in $N.(unit\ of\ length)^{-1}$. One can view a state of prestress as a new rest position. Hence, the force needed to create an elongation of 1 unit of length chosen in the prestress system is $F = k * 1 + F_0 > k * 1$. See figure below.

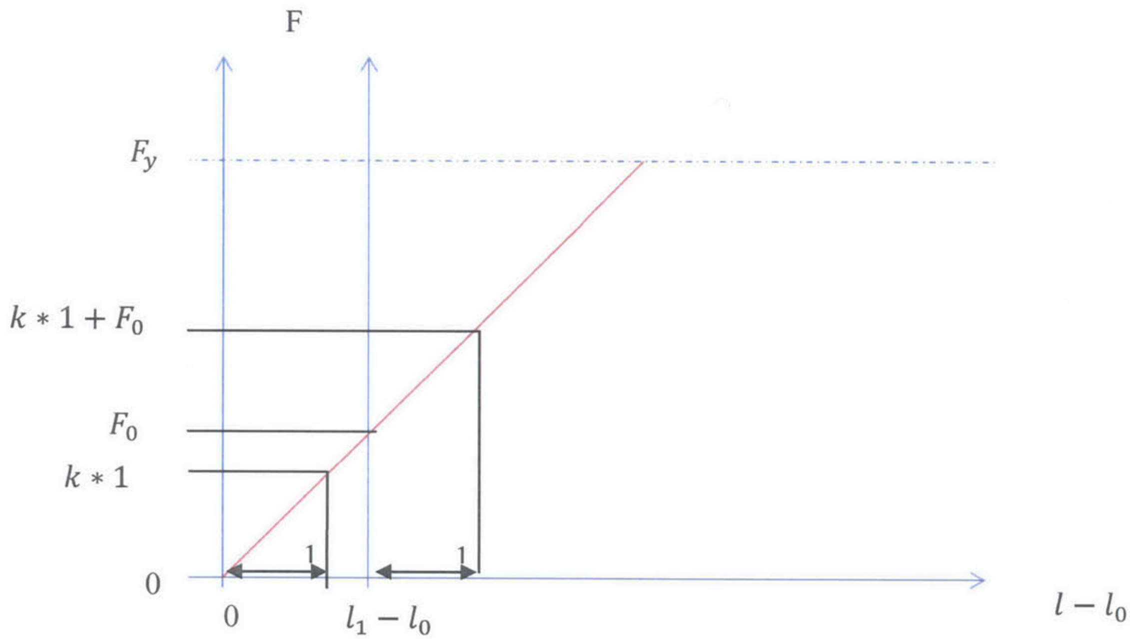

Figure 7 : Different state of stress for a spring element

Another advantage of prestress lies in the fact that it virtually increases the force domain a member can carry. In a prestressed concrete beam for instance, the bottom flange, which is supposed to carry tension when the beam is under a positive bending moment, is precompressed. This gives an extra capacity in tension. By knowing the forces in a system after application of the design loads, one could potentially design the initial state in order to minimize the cross-sectional area of the members. Say a particular member is supposed to carry $5kN$ of compression after the external loads are applied on the system. Starting with an initial pretension of $2.5kN$ reduces the absolute value of the force in the member by half (. But this only applies to bilateral truss members. Indeed, in order to symmetrize the loading on the member, it has to be able to carry both tension and compression.

1.2.3 Applications of tensegrity structures

Because of its aesthetically pleasing aspect, the first applications of tensegrity structures were artistic sculptures (e.g. Rainbow Arch by K. Snelson). Since cables do not need as much cross-section area in comparison with bars, a system in which struts form a discontinuous set will give the impression that compressive members are literally floating in the air. This is what K. Snelson meant by "floating compression".

Later, scientists set their sights on this specific class of structures. A famous application is the tensegrity model of the cell mechanics. Prof. Donald E. Ingber reviewed the evidences supporting the idea that the cytoskeleton in a cell would have a tensegrity architecture (Ingber, 2003). Figure 8 shows the main structural components in a cytoskeleton. On one hand, the Actin Microfilaments, in red on A and abbreviated MFs in B, are the analogous of the cables. On the other hand, the Microtubules, in green in A and abbreviated MTs in B, are the equivalent of the struts. Another important mechanical component is the Extracellular matrix, denominated ECM in B. The ECM is experiencing traction just like the attachments of a spider web would. The whole system is active as the prestress can be modified depending on the situation.

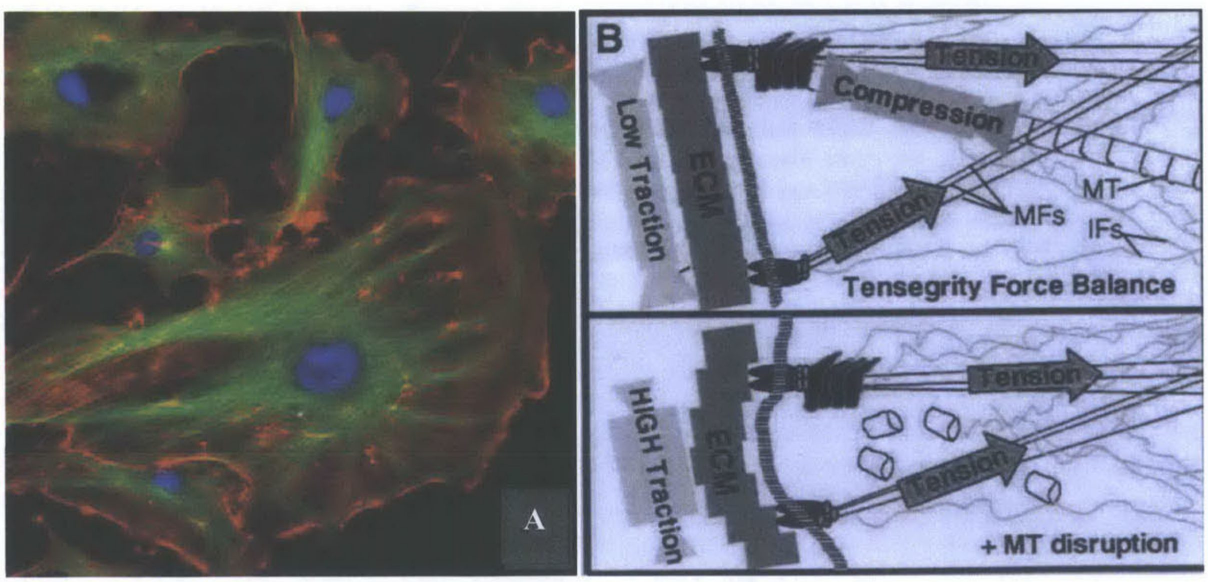

Figure 8 : Endothelial cells under the microscope (A) and tensegrity model (B) from (Ingber, 2003)

Other structures in life have been identified as tensegrity such that muscles-bones systems. Forecasting how prolific this concept would be, Prof. E. Ingber used the expression "Architecture of Life" (*Scientific American, 1998*). After that, only one step leads to biomimicry.

In Engineering, the two main fields that showed interest for the tensegrity concept are the aerospace sector and the civil sector. Except the pleasing architecture, one of the main advantages of this class of systems is their ability to change shapes without the need of a lot of energy. This supports the life architecture idea as one of the key concepts in Nature is the minimization of energy. Providing some energy and the right actuator, one can envision tensegrity deployable structures. See (Rhode-Barbarigos, Schulin, Bel Hadj Ali, Motro, & Smith, 2012) for a study of the deployment of a ring pedestrian bridge. Another advantage is the ability to support a multimodular architecture, i.e. a module is replicated, potentially at various scales, to compose a larger structure. This can potentially add some redundancy in the system.

1.3 Literature review on the optimization of articulated structures

Many papers have been published on the optimization of articulated structures (trusses or tensegrities). In most of them, see (Jarre, Kocvara, & Zowe, 1998) for instance, the geometry and the connectivity of a structure are given for the optimization problem. They deal with the question of finding the best load path by mapping a relevant portion of the space with fixed locations nodes and starting with a maximal connectivity. At every turn if a node and/or a member do not participate much, they are taken out of the problem. The geometry of the structure is then refined.

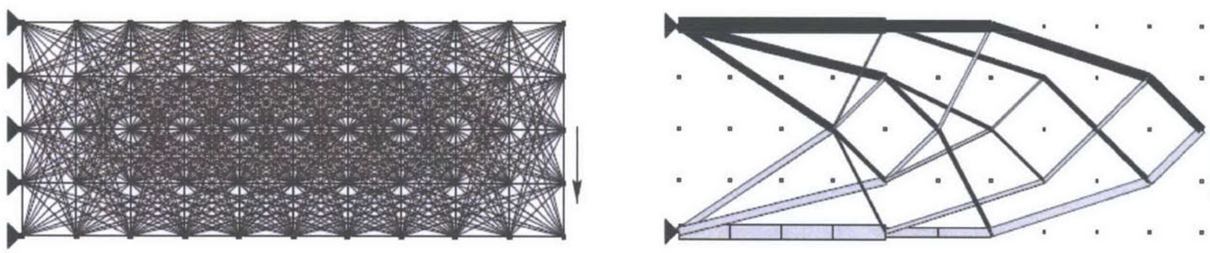

Figure 9 : Cantilever truss optimization (Jarre, Kocvara, & Zowe, 1998)

This approach works and one can easily see that if the mapping is fine, the solution obtained will be the good one in terms of geometry and connectivity. However, this creates a lot of variables and limits the search to a small area.

In the following, a new approach is considered where both geometry and connectivity are actually part of the optimization. A certain number of nodes have variable coordinates and the connectivity can be seen as a set of binary variables; one for each pair of nodes in the system.

2. Formulation of the optimization problem

In this section, the problem of the optimization of articulated structures is formulated, including tensegrity systems, so that it falls into the typical mathematical formalism of optimization.

2.1 Data and choice of the variables

Starting with a load-carrying problem such as the cantilever example of section 1.1, one needs to define what is given (data or parameters) and what is to be found (variables). In this section, the formulation for the general problem is presented.

The data that is assumed to be given:

- The forces applied and the coordinates of the application points in given coordinate system
- The supports provided and the coordinates of the support points in a given coordinate system
- The materials (and thus their properties) out of which the members will be made of

The problem remains very general this way and many structural systems could potentially be considered to carry the load to the supports.

Since the scope of work for this thesis is to study how tensegrity systems could potentially provide a good solution in structural engineering, throughout the document we will compare the solutions obtained with this class of structures against the ones obtained with regular truss systems.

The decisions to be made to define a viable structure are then:

	Regular Truss	Tensegrity
Geometry	Choose how many nodes to add to the problem and their coordinates.	Choose how many nodes to add to the problem and their coordinates.
Connectivity	For each pair of nodes choose if a member joins them.	For each pair of nodes choose if a member joins them and if there is whether it is a cable or a strut.
Scale	For each member choose the cross-sectional area.	For each member choose the cross-sectional area and the prestress

Table 1 Comparison of the design steps for truss and tensegrity

In a nutshell, the tensegrity problem is the same as the truss with two extra decisions: the choice between cables and bars and what prestress to put in the members.

To represent these decisions in the optimization process, there are several options in terms of choice of variables. For instance, the prestress in a member could be represented either by its rest length l_0, or the actual prestress force $F_0 = k(l - l_0)$; where k is the axial rigidity of the member and l is the length of the member in the initial state.

2.1.1 Geometry variables

Let $\boldsymbol{N}$ be the matrix of the nodes coordinates in the chosen coordinate system. At every line we find the three, or two coordinates if we are in 2D, of a certain node. Some of the nodes are the given supports and load application nodes. Let n be the number of added nodes to the system and p be the total number of nodes. The coordinates of these n nodes are the geometric variables.

In order to avoid degenerative cases we forbid two nodes to have the same coordinates. Hence, no member will have a length of 0.

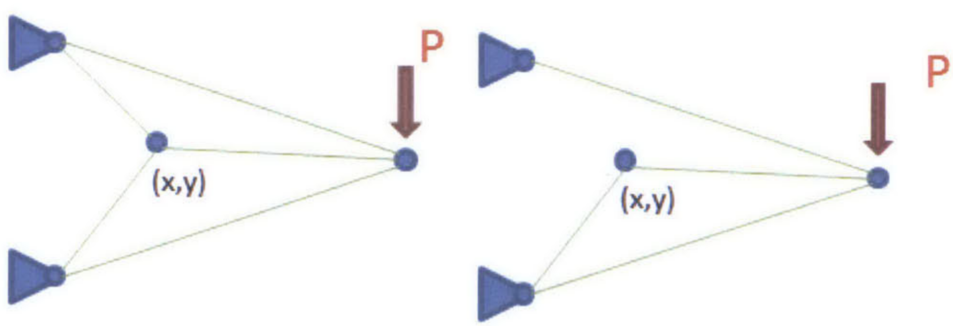

Figure 10 : Two configurations with one added point and different connectivities

2.1.2 Connectivity variables

One way to represent a connection between two nodes is to associate a binary variable for every pair of nodes. If we number the elements in the following way:

$$\zeta : \quad \{(i,j) \in [\![1,p]\!]^2 \mid i < j\} \to [\![1, \tfrac{p(p-1)}{2}]\!]$$
$$(i,j) \mapsto h = \zeta(i,j) = p(i-1) - \frac{(i-1)i}{2} + j - i$$

The connectivity space is then $\mathbb{C}_p = \{0,1\}^{[\![1,\frac{p(p-1)}{2}]\!]}$. For an element of $\mathbb{C}_p$, having a 1, a 0, at place h means there is, respectively there is not, a member joining the pair of nodes (i,j) such that $h = p(i-1) - \frac{(i-1)i}{2} + j - i$ and $1 \leq i < j \leq p$. For tensegrity systems, the connectivity space is bigger: $\mathfrak{C}_p = \{-1,0,1\}^{\left[\!\left[1,\frac{p(p-1)}{2}\right]\!\right]}$. 1 could be associated with cables and -1 with bars. The total number of elements in a system is then:

$$m = \sum_h |\theta_h| \ for \ (\theta_h) \in \mathbb{C}_p \ or \ \mathfrak{C}_p$$

A necessary condition for an articulated system to be stable is $3p - s \leq m$, where s is the number of supports provided to the system and m is the total number of elements. This stability condition implies that only the following subset of $\mathbb{C}_p$ or $\mathfrak{C}_p$ is worth looking at:

$$D_p = \left\{ (\theta_h) \in \mathbb{C}_p \ or \ \mathfrak{C}_p \ \mid \ \sum_h |\theta_h| \geq 3p - s \right\}$$

The cardinal number of this subset is:

$$\sum_{k=3p-s}^{\frac{p(p-1)}{2}} \binom{\frac{p(p-1)}{2}}{k}$$

Please note, factors 3 become 2 for plane structures.

In the following, though, I use an indirect method to represent the connectivity of the nodes.

For a member h, let $\boldsymbol{C}^{(h)}$ be the member's connectivity matrix with respect to the whole system. Its number of rows is equal to the total number of members and its number of columns is equal to the total number of nodes. The general term of this matrix is:

$$\boldsymbol{C}_{ab}^{(h)} = \begin{cases} -1 \ if \ a = h \ and \ b = i \ such \ that \ \ h = \zeta(\mathrm{i},\mathrm{j}) \\ \ 1 \ \ if \ a = h \ and \ b = j \ such \ that \ h = \zeta(\mathrm{i},\mathrm{j}) \\ \ 0 \qquad\qquad\qquad otherwise \end{cases}$$

The order of the pair (i,j) matters as we assume the member's orientation is i towards j. The connectivity matrix of the structure is then:

$$\boldsymbol{C} = \sum_h \boldsymbol{C}^{(h)}$$

This matrix has only two non-zero coefficients on each line. For tensegrity structures, we add a diagonal matrix $\boldsymbol{\varepsilon}$ with -1 or $+1$ on the diagonal deal with the choice between bar and cable for each element.

2.1.3 Scale variables

Regarding scale variables, we will use a diagonal matrix $\boldsymbol{A}$ (living in a space isomorphic to $(\mathbb{R}_+^*)^m$) for which every coefficient on the diagonal represents the resisting cross-sectional area of a member. For tensegrity structures only, we add a diagonal matrix $\boldsymbol{l}^{(0)}$ (also living in a space isomorphic to $(\mathbb{R}_+^*)^m$) constructed in a similar manner than $\boldsymbol{A}$ with the rest length of the members on the diagonal to represent the prestress. The relationship between $\boldsymbol{F_0}$, diagonal matrix with the prestress forces in the members, and $\boldsymbol{l}^{(0)}$ is the following:

$$\boldsymbol{F_0} = \left(\frac{\varepsilon + \boldsymbol{I}^{mm}}{2} E_c - \frac{\varepsilon - \boldsymbol{I}^{mm}}{2} E_b\right) \boldsymbol{A} \left(\boldsymbol{l}^{(0)}\right)^{-1} \left(\boldsymbol{l} - \boldsymbol{l}^{(0)}\right)$$

E_b and E_c being the Young's modulus of the materials of which the bars and cables are made of.

2.1.4 Note on the configurations

For a truss system, two configurations can be distinguished: the initial and the deformed one, obtained after application of the external loads.

For a tensegrity system now, there are three configurations. The "pre-initial" configuration is the one for which the prestress has not been applied yet. The initial configuration is the one in state of prestress equilibrium, which can be seen as a deformed configuration obtained from the "pre-initial" state by applying the prestress loads. Similarly to a truss, the final configuration corresponds to the deformed initial system under the external loads.

In some papers on tensegrity structures the three states of a system are considered. Since knowledge of the "pre-initial" configuration's geometry is not important for the optimization problem, in the following I disregard it. What matters is the quantification of the prestress, which is represented by the variables $\boldsymbol{l}^{(0)}$, and to ensure the initial configuration is in prestress equilibrium, which is enforced by a constraint (see section 2.2.2.3).

2.2 Formulation of the optimization problem

Notation precision: In the following, when operators are applied to diagonal matrices, they are to be understood as the operation being applied to every diagonal coefficient.

2.2.1 Objective function

The matrix composed of the coordinates of the oriented vectors corresponding to the members is $\boldsymbol{CN}$. Hence, the diagonal matrix containing the length of all the members on its diagonal is:

$$\boldsymbol{l} = \sqrt{\sum_h (\boldsymbol{C}^{(h)}\boldsymbol{N})(\boldsymbol{C}^{(h)}\boldsymbol{N})^T}$$

The objective function we want to minimize can now be defined; it is the mass of the system. Assuming a constant mass density, the volume can be substituted to the mass as the objective function:

$$V = \begin{cases} Tr(\boldsymbol{l}\,\boldsymbol{A}) & \textit{for regular truss structures} \\ Tr\left(\boldsymbol{l}^{(0)}\boldsymbol{A}\right) & \textit{for tensegrity structures} \end{cases}$$

2.2.2 Constraints

A structure constructed as above is viable if and only if it meets the control requirements. This includes both strength and motion specifications. Indeed, we do not want any member to fail or the structure to move too much. These conditions translate into constraints on the variables defined in section 2.1.

In the following, the small perturbations assumption is made. This allows the linearization of the equilibrium equations, which can be written on the initial configuration, and the use of the linearized model for the members' mechanical behavior. Dynamic could be considered if some of the motion prescription take the form of a maximum acceleration but, for the scope of this thesis we will limit ourselves to a static model. To derive the equilibrium equations, I use the stiffness method (see Appendix 1).

2.2.2.1 Equilibrium equation

The static equilibrium equation for both a truss structure and a tensegrity structure is $\underline{\boldsymbol{f}} = \underline{\underline{\boldsymbol{K}}}\,\underline{\boldsymbol{U}}$ (see Appendix 1). However, the only change is in the expression of the stiffness matrix $\underline{\underline{\boldsymbol{K}}}$ due to the difference in stiffness between the two types of elements used in tensegrity.

The decomposition $\underline{\boldsymbol{f}}=\underline{\boldsymbol{Q}}+\underline{\boldsymbol{R}}$, with $\underline{\boldsymbol{Q}}$ being the applied external forces and $\underline{\boldsymbol{R}}$ being the reactions forces of the supports corresponding to these external loads, holds for both trusses and tensegrities. Indeed, one could write $\underline{\boldsymbol{f}}=\underline{\boldsymbol{Q}}+\underline{\boldsymbol{R}}+\underline{\boldsymbol{R_0}}-\underline{\boldsymbol{Q_0}}$, with $\underline{\boldsymbol{Q_0}}$ being the prestress loads and $\underline{\boldsymbol{R_0}}$ the corresponding reaction, but, since a tensegrity is in prestressed equilibrium $\underline{\boldsymbol{R_0}} - \underline{\boldsymbol{Q_0}} = \boldsymbol{0}$.

From the stiffness, we get two outputs: the generalized displacement vector $\underline{\boldsymbol{U}}$ and the diagonal matrix with on the diagonal the forces of the members in the deformed configuration $\boldsymbol{F}$.

2.2.2.2 Constraints

There is a wide range of constraints that can be applied to the system. Here, I select only a few that are essential.

- Stability constraint

For a structure to be viable it must be stable. The mathematical expression of this requirement is:

$$\det(\boldsymbol{K_{MM}}) \neq 0$$

Where $\boldsymbol{K_{MM}}$ is the extracted matrix from the system stiffness matrix corresponding to the non-fixed degrees of freedom.

However, since a non-equality constraint does not fall into the typical mathematical framework of optimization, we have two options:

- Either modify the constraint in $\omega - |\det(\boldsymbol{K}_{MM})| \leq 0$ with a parameter ω chosen sufficiently small.

- Disregard this constraint and modify the stiffness method so that it returns infinite displacements if the structure is not stable.

In the following, we choose the second option.

- Strength constraints – Yielding of the members

This constraint represents the fact that no member in the structure is allowed to yield. The mathematical expression for a truss is:

$$\mathrm{abs}(\boldsymbol{F})\boldsymbol{A}^{-1} - f_y \boldsymbol{I}^{mm} \leq \boldsymbol{0}$$

For a tensegrity, this has to be true for the initial configuration as well as for the deformed configuration:

$$\mathrm{abs}(\boldsymbol{F})\boldsymbol{A}^{-1} - \left(\frac{\boldsymbol{\varepsilon} + \boldsymbol{I}^{mm}}{2} f_{y,c} - \frac{\boldsymbol{\varepsilon} - \boldsymbol{I}^{mm}}{2} f_{y,b}\right) \leq \boldsymbol{0}$$

$$\mathrm{abs}(\boldsymbol{F_0})\boldsymbol{A}^{-1} - \left(\frac{\boldsymbol{\varepsilon} + \boldsymbol{I}^{mm}}{2} f_{y,c} - \frac{\boldsymbol{\varepsilon} - \boldsymbol{I}^{mm}}{2} f_{y,b}\right) \leq \boldsymbol{0}$$

Where $f_{y,c}$ and $f_{y,b}$ are the yield stresses of the bars and cables respectively. These values could potentially be discounted to account for some safety.

- Strength constraints – Buckling of the compressive members

This constraint represents the fact that no struts in the structure is allowed to buckle. The mathematical expression for a truss is:

$$\max(-\boldsymbol{F}, \boldsymbol{0}) - \pi^2 E \boldsymbol{I} \boldsymbol{l}^{-2} \leq \boldsymbol{0}$$

For a tensegrity, the constraints must be verified for both the initial and the deformed configuration:

$$\max(-\boldsymbol{F}, \boldsymbol{0}) - \pi^2 E_b \boldsymbol{I} {\boldsymbol{l}^{(0)}}^{-2} \leq \boldsymbol{0}$$

$$\max(-\boldsymbol{F_0}, \boldsymbol{0}) - \pi^2 E_b \boldsymbol{I} {\boldsymbol{l}^{(0)}}^{-2} \leq \boldsymbol{0}$$

In all these expressions, we have used the diagonal matrix $\boldsymbol{I}$ with the inertia of the members as diagonal coefficients.

One could argue buckling is a false problem as the inertia could be adjusted by shaping the bars appropriately. Indeed, the inertia represents how far the cross-sectional area is away from the neutral axis. In an optimal behavior of compressive members, the buckling force would be equal to the yielding force so that there is no wasted material. For a member with a fixed length and cross sectional area (to prevent yielding), one could play with the distance of this area from the neutral axis to get the right inertia.

In pure compression, a necessary condition for optimality in buckling is a member which has revolution symmetry about its neutral axis. Indeed, if it was not the case there would be a privileged buckling direction. Easy solutions for compressive members' shape would then be solid rods or circular tubes. We have the two following relationships for these two cases:

Solid rod: $I = \pi \frac{R^4}{4} = \frac{A^2}{4\pi}$ Circular tube with thin walls: $I = \pi R^3 t = \frac{A^3}{8\pi^2 t^2}$

Where I is the inertia of the section, R is the radius of the section, A is the cross-sectional area and t is the thickness of the walls for the tube case. For a fixed area, one could adjust the value of the thickness to meet the buckling criterion. The smaller the thickness, the larger the inertia would be but, the tradeoff is a large radius ($R = \frac{A}{2\pi t}$).

This is only looking at constant inertia members which are not an optimum. Indeed, cigar shapes, for instance, perform better to prevent the first buckling mode. One could refine the shape further but, it is an independent problem in itself.

Two options are available for the optimization problem:

- Consider buckling constraints with a specific type of compressive members' geometry in which case more complex geometries, like a tube, would add more variables to the problem.
- Disregard buckling constraints assuming this problem will be solved independently afterwards by adjusting the geometry of each compressive member.

In the following, I use the first option and assume struts are solid rods to minimize the number of variables.

- Motion constraints – Displacement

This constraint represents the control of the displacement of the structure.

The main output from the stiffness method (see Appendix 1) is the generalized displacement vector $\underline{\boldsymbol{U}}$ with the components of the displacements of each node in the structure. Given a corresponding specified vector of maximum displacement for each degree of freedom $\underline{\boldsymbol{U_d}}$, this constraint can be expressed:

$$\text{abs}(\underline{\boldsymbol{U}}) - \underline{\boldsymbol{U_d}} \leq 0$$

- Tensegrity specific constraints – Prestressed equilibrium

A tensegrity system must be in equilibrium in the initial configuration under the prestress loads. This translates into a constraint on the set of initial forces in the members:

$$\underline{\boldsymbol{Q_0}}_M = \left(\underline{\boldsymbol{Q_0}}_{\sigma(i)}\right) = \mathbf{0}$$

Where $\underline{\boldsymbol{Q_0}}$ is the generalized prestress load vector and σ is the permutation of $[\![1,3p]\!]$ introduced in Appendix 1. With the notation of Appendix1, $\underline{\boldsymbol{Q_0}}$ is derived from $\boldsymbol{F_0}$ with the following formula:

$$\underline{\boldsymbol{Q_0}} = \sum_{a=1}^{3} \sum_{\substack{h=1 \\ h=\zeta(i,j)}}^{m} \left(\boldsymbol{E}_{3j-3+a,h}^{3p\,m} - \boldsymbol{E}_{3i-3+a,h}^{3p\,m}\right)\boldsymbol{F_0}\boldsymbol{l}^{-1}\boldsymbol{CNE}_{1a}^{13}$$

An articulated structure is prestressable if and only if an autoequilibrated force field exists. For this to be possible, the system has to be hyperstatic. Hence, an alternative to deal with this constraint is to consider only a number of prestress force variables equal to the hyperstaticity of the system and enforce equilibrium to obtain the prestress forces in the other members. This method has the advantage of removing the only equality constraint we had so far and to decrease the number of variables.

- Tensegrity specific constraints – Unilateral member

As mentioned before even though bars have a bilateral behavior in the following we assume they cannot carry tension so that cables are selected. Hence, the constraints to ensure cables, struts, carry only tension, compression respectively, are:

$$\left(\frac{\boldsymbol{\varepsilon} - \boldsymbol{I}^{mm}}{2}\boldsymbol{F} - \frac{\boldsymbol{\varepsilon} + \boldsymbol{I}^{mm}}{2}\boldsymbol{F}\right) \leq \mathbf{0}$$

$$\left(\frac{\boldsymbol{\varepsilon} - \boldsymbol{I}^{mm}}{2}\boldsymbol{F_0} - \frac{\boldsymbol{\varepsilon} + \boldsymbol{I}^{mm}}{2}\boldsymbol{F_0}\right) \leq \mathbf{0}$$

- Architectural constraints

One could potentially add architectural constraint. For instance, on a tensegrity system we might want to impose the radius of the bars to be sufficiently bigger compared to the radius of the cables to have the "floating compression" feel described by Snelson. Mathematically, it could look like (with the solid rods assumption):

$$\beta \max_{h\in[\![1,m]\!]}(\boldsymbol{\varepsilon}_{hh}\boldsymbol{A}_{hh}) - \max_{h\in[\![1,m]\!]}(\min(\boldsymbol{\varepsilon}_{hh}\boldsymbol{A}_{hh}, 0)) \leq 0$$

This states that the lowest radius among the bars is sufficiently larger than the maximum radius of the cables (as controlled by the parameter $\beta > 0$).

Another architectural constraint that could be imposed is having members that are slender enough. It could be represented mathematically by (with the solid rods assumption):

$$\sqrt{\boldsymbol{A}}\boldsymbol{l}^{-1} - \delta\boldsymbol{I}^{mm} \leq \mathbf{0}$$

$\delta > 0$ is a slenderness ratio parameter to be specified.

- Feasibility constraints

Feasibility constraints could potentially account for construction constraints or a way to enforce realistic solutions (e.g. avoiding clash between members in 3D). One could specify a minimum length $\varphi \geq 0$ for the members and the constraint would be:

$$\varphi \boldsymbol{I}^{mm} - \boldsymbol{l} \leq \boldsymbol{0}$$

2.2.3 Important remarks on the formulation

In its current state the formulation has several flaws.

2.2.3.1 Rest lengths

Rest lengths are not ideal for direct use as variables if we plan pursuing in a numerical optimization on a computer. Indeed, the rest lengths variables are not allowed to vary a lot. To understand this let us write the yielding and unilateral member constraint differently. Let $h \in [\![1, m]\!]$ be a member number.

If $\boldsymbol{\varepsilon}_{hh} = -1$, member h is a strut and needs to verify:

$$\boldsymbol{l}_{hh} \leq \boldsymbol{l}_{hh}^{(0)} \leq \frac{\boldsymbol{l}_{hh}}{\left(1 - \frac{f_{y,b}}{E_b}\right)}$$

With $f_{y,b} = 235MPa$ and $E_b = 210{,}000MPa$ the upper bound is equal to $1.00112 * \boldsymbol{l}_{hh}$.

If $\boldsymbol{\varepsilon}_{hh} = +1$, member h is a cable and needs to verify:

$$\frac{\boldsymbol{l}_{hh}}{\left(1 + \frac{f_{y,c}}{E_c}\right)} \leq \boldsymbol{l}_{hh}^{(0)} \leq \boldsymbol{l}_{hh}$$

With $f_{y,c} = 1GPa$ and $E_c = 170GPa$ the lower bound is equal to $0.994152 * \boldsymbol{l}_{hh}$.

$\boldsymbol{l}_{hh}$ is a function of the geometric variables (coordinates of the nodes that are added to the structure) and the interval of variation for $\boldsymbol{l}_{hh}^{(0)}$ will increase for large values of $\boldsymbol{l}_{hh}$ but it is not a safe choice. As a result of this remark, when $\boldsymbol{l}^{(0)}$ is multiplied or divided it will be replaced by $\boldsymbol{l}$. In particular, the expression of the volume of the structure becomes the same for a trusses and tensegrities. The axial rigidity of a member is also simplified.

Additionally, $\boldsymbol{F_0}$ will be preferred to $\boldsymbol{l}^{(0)}$ as the variable to represent prestress in tensegrity structures. Indeed, a small change in length will induce large forces in the members. Optimization algorithms can operate at a resolution that captures the variation of $\boldsymbol{F_0}$.

2.2.3.2 Closure of the variables' space

In an optimization problem, the solution might be reached on the border of the variable space. For instance, $x \mapsto \frac{1}{x}$ defined on $]1,3[$ is maximum in 1 and minimum in 3. Both of these points are not in the variable space. If we want the solutions to be in the feasible set of variables, the variables' space has to be closed. This is why all the constraints are defined with equality or less than or equal inequality instead of strictly less than.

In our formulation of the problem, the variables' space can be seen as the Cartesian product of several sets:

For every $n \in \mathbb{N}$,

Truss: $$\left((\theta_h),(x_i,y_i,z_i),(\boldsymbol{A}_{hh})\right) \in \{0,1\}^{\left[\!\left[1,\frac{p(p-1)}{2}\right]\!\right]} \times G \times (\mathbb{R}_+^*)^m$$

Tensegrity: $$\left((\theta_h),(x_i,y_i,z_i),(\boldsymbol{A}_{hh}),\left(\boldsymbol{F_0}_{hh}\right)\right) \in \{-1,0,1\}^{\left[\!\left[1,\frac{p(p-1)}{2}\right]\!\right]} \times G \times (\mathbb{R}_+^*)^m \times (\mathbb{R})^m$$

Where $G = \{(x_i,y_i,z_i) \in (\mathbb{R}^3)^n \mid \forall\, h \in [\![1,m]\!], \boldsymbol{l}_{hh} \neq 0\}$.

G and $(\mathbb{R}_+^*)^m$ are not closed which could cause a stability issue in the resolution of the problem. This could potentially be resolved by imposing a constraint on the length of the member (see section 2.2.2.2) and by modifying the area space to $([a_0,+\infty[)^m$ with a_0 a minimum area parameter to be chosen. However, by doing so we might miss the optimum if the minimum length and/or the minimum area chosen are too small. I will refer to this formulation as $(\mathcal{F}_1)$.

A slightly different formulation that we are going to call $(\mathcal{F}_2)$ of the problem could be considered. Instead of deciding whether a member is joining every pair of nodes, one could assume a maximal connectivity, i.e. all nodes are connected to each other, and allow $\boldsymbol{A}$ to live in$(\mathbb{R}_+)^{\frac{p(p-1)}{2}}$.

For every $n \in \mathbb{N}$,

Truss: $$\left((x_i,y_i,z_i),(\boldsymbol{A}_{hh})\right) \in (\mathbb{R}^3)^n \times (\mathbb{R}_+)^{\frac{p(p-1)}{2}}$$

Tensegrity: $$\left((\theta_h),(x_i,y_i,z_i),(\boldsymbol{A}_{hh}),\left(\boldsymbol{F_0}_{hh}\right)\right) \in \{-1,1\}^{\left[\!\left[1,\frac{p(p-1)}{2}\right]\!\right]} \times (\mathbb{R}^3)^n \times (\mathbb{R}_+)^{\frac{p(p-1)}{2}} \times (\mathbb{R})^{\frac{p(p-1)}{2}}$$

The variables' space is now closed and there are actually less variables than in the previous formulation. The tradeoff, however, is the need to adjust the method used to solve the equilibrium equations.

2.2.3.3 Existence of the solution

Before actually trying to look for a solution, existence of a solution has to be proven. For every $n \in \mathbb{N}$ and every (θ_h), the resulting objective function is a continuous function of the variables $\left((x_i, y_i, z_i), (\boldsymbol{A}_{hh}), (\boldsymbol{F_0}_{hh})\right)$.

$(\boldsymbol{F_0}_{hh})$ lives in a compact space due the tensegrity constraints (see section 2.2.2.2). With formulation $(\mathcal{F}_1)$, the objective function is coercive in both the geometric variables (x_i, y_i, z_i) and the cross-sectional area variables $(\boldsymbol{A}_{hh})$; when $\left\|\left((x_i, y_i, z_i), (\boldsymbol{A}_{hh})\right)\right\| \to +\infty$ we have $V \to +\infty$.

With formulation $(\mathcal{F}_2)$ however, the objective function is not coercive. Indeed, if one member has a length of 0 the corresponding area variable can go to infinity without affecting the volume of the system. Hence, there is no point looking for a minimum with this formulation as there is an infinite number of them.

Since there is a finite number of (θ_h) for every $n \in \mathbb{N}$ and for all the reasons that have been mentioned above, we know that for every $n \in \mathbb{N}$ an optimum configuration exists. The sequence of the corresponding minimum volumes can be called $(V_n)_{n\in\mathbb{N}}$. Optimizing a structure is then reduced to the study of this sequence.

2.2.4 Summary

The mathematical formulation of the optimization problem is for every $n \in \mathbb{N}$:

For every $n \in \mathbb{N}$, solve:

$$\begin{cases} \min V(X) \\ X \in S \\ g_j(X) \le 0 \; for \; j \in [\![1, q_{in}]\!] \\ h_i(X) = 0 \; for \; i \in [\![1, q_{eq}]\!] \end{cases}$$

Where X is the global variable for the problem and S is the truss or tensegrity variables' space as in section 2.2.3.2. (g_j) and (h_i) are a selection of inequality and equality constraints to be chosen. The table below summarizes the one that were introduced previously; some of them are mandatory (underlined) and the others are optional.

	Truss	Tensegrity
Variables	$\left((\theta_h), (x_i, y_i, z_i), (\boldsymbol{A}_{hh})\right)$	$\left((\theta_h), (x_i, y_i, z_i), (\boldsymbol{A}_{hh}), (\boldsymbol{F_0}_{hh})\right)$
Variables' space	$\{0,1\}^{[\![1, \frac{p(p-1)}{2}]\!]} \text{ x G x } ([a_0, +\infty[)^m$	$\{-1,0,1\}^{[\![1, \frac{p(p-1)}{2}]\!]} \text{ x G x } ([a_0, +\infty[)^m \text{ x } (\mathbb{R}_+)^m$
Objective function	$Tr(\boldsymbol{l}\,\boldsymbol{A})$	$Tr(\boldsymbol{l}\,\boldsymbol{A})$
<u>Stability constraint</u>[2]	-	-

[2] Included by modifying the stiffness method (see section 2.2.2.2)

Yielding constraint	$\mathrm{abs}(\boldsymbol{F})\boldsymbol{A}^{-1} - f_y \boldsymbol{I}^{mm} \leq \boldsymbol{0}$	$\mathrm{abs}(\boldsymbol{F})\boldsymbol{A}^{-1} - \left(\frac{\boldsymbol{\varepsilon} + \boldsymbol{I}^{mm}}{2} f_{y,c} - \frac{\boldsymbol{\varepsilon} - \boldsymbol{I}^{mm}}{2} f_{y,b}\right) \leq \boldsymbol{0}$ $\mathrm{abs}(\boldsymbol{F_0})\boldsymbol{A}^{-1} - \left(\frac{\boldsymbol{\varepsilon} + \boldsymbol{I}^{mm}}{2} f_{y,c} - \frac{\boldsymbol{\varepsilon} - \boldsymbol{I}^{mm}}{2} f_{y,b}\right) \leq \boldsymbol{0}$
Buckling constraint[3]	$\max(-\boldsymbol{F}, \boldsymbol{0}) - \pi^2 E \boldsymbol{I} \boldsymbol{l}^{-2} \leq \boldsymbol{0}$	$\max(-\boldsymbol{F}, \boldsymbol{0}) - \pi^2 E_b \boldsymbol{I} \boldsymbol{l}^{-2} \leq \boldsymbol{0}$ $\max(-\boldsymbol{F_0}, \boldsymbol{0}) - \pi^2 E_b \boldsymbol{I} \boldsymbol{l}^{-2} \leq \boldsymbol{0}$
Displacement constraint	$\mathrm{abs}(\underline{\boldsymbol{U}}) - \underline{\boldsymbol{U_d}} \leq 0$	$\mathrm{abs}(\underline{\boldsymbol{U}}) - \underline{\boldsymbol{U_d}} \leq 0$
Prestressed equilibrium	-	$\boldsymbol{Q}_{\boldsymbol{0}_M} = \left(\boldsymbol{Q}_{\boldsymbol{0}_{\sigma(i)}}\right) = \boldsymbol{0}$
Unilateral member	-	$\left(\frac{\boldsymbol{\varepsilon} - \boldsymbol{I}^{mm}}{2} \boldsymbol{F} - \frac{\boldsymbol{\varepsilon} + \boldsymbol{I}^{mm}}{2} \boldsymbol{F}\right) \leq \boldsymbol{0}$ $\left(\frac{\boldsymbol{\varepsilon} - \boldsymbol{I}^{mm}}{2} \boldsymbol{F_0} - \frac{\boldsymbol{\varepsilon} + \boldsymbol{I}^{mm}}{2} \boldsymbol{F_0}\right) \leq \boldsymbol{0}$
Floating compression	-	$\beta \max_{h \in [\![1,m]\!]}(\boldsymbol{\varepsilon}_{hh} \boldsymbol{A}_{hh}) - \max_{h \in [\![1,m]\!]}(\min(\boldsymbol{\varepsilon}_{hh} \boldsymbol{A}_{hh}, 0)) \leq 0$
Slenderness constraint	$\sqrt{\boldsymbol{A}} \boldsymbol{l}^{-1} - \delta \boldsymbol{I}^{mm} \leq \boldsymbol{0}$	$\sqrt{\boldsymbol{A}} \boldsymbol{l}^{-1} - \delta \boldsymbol{I}^{mm} \leq \boldsymbol{0}$
Minimum length[4]	$\varphi \boldsymbol{I}^{mm} - \boldsymbol{l} \leq \boldsymbol{0}$	$\varphi \boldsymbol{I}^{mm} - \boldsymbol{l} \leq \boldsymbol{0}$

Table 2 Summary of the variables and expressions of the constraints and the objective function

[3] This assumes no optimization of the cross-section is conducted (see section 2.2.2.2)
[4] To ensure closure of the variables' space (see section 2.2.3.2)

3. First examples

As a first experiment, I study in this section the first two cases, n=0 and n=1, for both regular trusses and tensegrities with a typical cantilever situation (see Figure 1) in 2D. This allows the derivation of preliminary results and comparison of tensegrity and truss performance. I only consider the mandatory constraints (see previous section).

When numerical applications are done, the following set of data would always be used:

- Applied Force:

$$P = 3kN$$

- Geometry:

$$L = H = 50cm$$

- Mechanical properties for the struts:

$$E_b = 210GPa = 21{,}000kN.cm^2$$
$$f_{yb} = 235MPa = 23.5kN.cm^2$$

- Mechanical properties for the cables:

$$E_c = 170GPa = 17{,}000kN.cm^2$$
$$f_{yc} = 1000MPa = 100kN.cm^2$$

- Displacement constraint factor:

$$\alpha = 360$$

For a problem with trusses, we will use only struts that can take both tension whereas for a tensegrity arrangement struts carrying compression only and cables carrying tension only will be used.

3.1 Truss optimization – No points added (n=0)

In this case we don't have any geometric variables as we do not add any point to the problem. Hence, we are left with a classic structural engineering problem where we need to size the cross-section of the members as per the different constraints.

The optimization problem for an articulated structure as formulated in section 2 requires the specification of the supports' coordinates. One might argue the supports' coordinates matter and he would be right. Here, it is clear that there is an optimal configuration where the depth and the location of the supports with the respect to the $y = 0$ line are optimal. The depth will have to be big enough so that it decreases the required cross-sectional areas of the members but small enough so that their lengths do not increase too much. Because of the asymmetry caused by the buckling constraint, the bottom support will tend to be as close as possible to the $y = 0$ line without increasing the force in the bottom member too much. But these considerations depend on how much force is applied. For the sake of this section argument, we will then stick with the fixed supports as defined below.

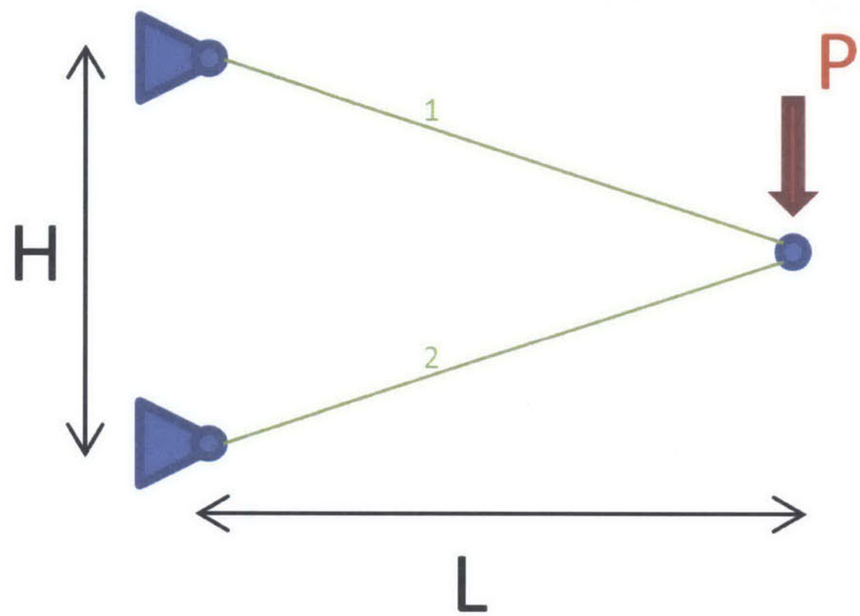

Figure 11: Cantilever truss problem n=0

Let A_1 and A_2 be the cross-sectional areas of members 1 and 2 respectively. This system is internally isostatic and the forces in the members are $F_1 = P\frac{\sqrt{\left(\frac{H}{2}\right)^2+L^2}}{H}$ and $F_2 = -P\frac{\sqrt{\left(\frac{H}{2}\right)^2+L^2}}{H}$.

We now impose the constraints:

- Yield:

$$\left|\frac{F_i}{A_i}\right| - f_y \leq 0, \qquad i = 1,2$$

$$\frac{A_{iy}}{A_i} \leq 1, \qquad i = 1,2$$

Where we have defined the parameters $A_{iy} = \frac{|F_i|}{fy}$ for $= 1,2$.

- Buckling:

$$-F_i - \frac{\pi^2 E I_i}{l_i^2} \leq 0, \qquad i = 1,2$$

Where I_i and l_i are respectively the inertia and the length of member i. In the case of solid rods, we have $I = \frac{A^2}{4\pi}$, hence the general formula can be simplified and we can define the buckling area parameters $A_{ib} = 2l_i\sqrt{\frac{\max(-F_i,0)}{\pi E}}$ for $i = 1,2$.

$$\frac{A_{ib}}{A_i} \leq 1, \qquad i = 1,2$$

- Displacement at the tip:

Equating the external energy provided to the system to the strain energy we get:

$$\frac{1}{P}\left(\frac{F_1^2}{k_1} + \frac{F_2^2}{k_2}\right) - u_d \leq 0$$

$$\frac{1}{P}\left(\frac{l_1F_1^2}{EA_1} + \frac{l_2F_2^2}{EA_2}\right) - u_d \leq 0$$

Where u_d is the maximum allowable displacement at the tip; typically $u_d = \frac{L}{\alpha}$ with α ranging from 200 to 500. Again we rewrite our constraint in an adimensional expression:

$$\frac{A_{1d}}{A_1} + \frac{A_{2d}}{A_2} \leq 1$$

Where the displacement area parameters are $A_{id} = \frac{l_iF_i^2}{PEu_d}$.

Physically, the constraints state that no member should have an area too small. Because the two members have the same length, the optimization of the volume of the system is equivalent to the optimization of the sum of the area of the two members: $A_1 + A_2$. Hence, we want A_1 and A_2 as small as possible as per the constraints. The unconstrained minimum for the volume function is obviously $A_1 = A_2 = 0$. If the displacement constraint is very lax, we get $A_1 = A_{1y}$ and $A_2 = \max(A_{2y}, A_{2b})$. When the displacement constraint gets more stringent however, this affects the areas to be chosen. Below is a graphic representation of the optimization.

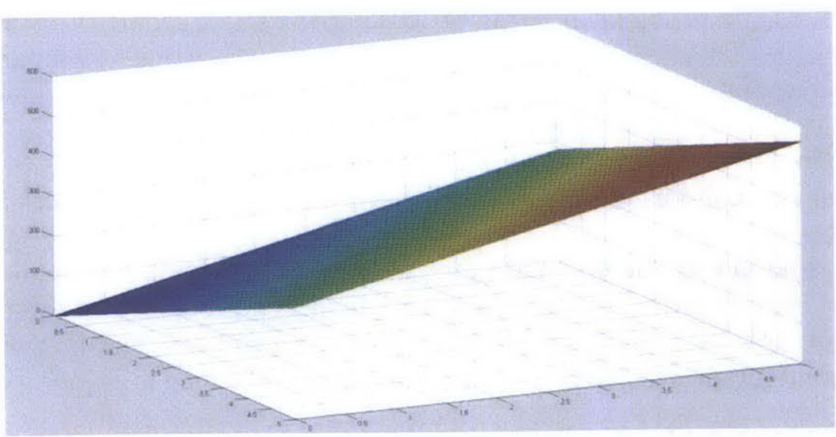

Figure 12: Surface plot of the volume function

For the numerical application, we use the values specified at the beginning of section 3. Looking at the feasible set of solutions in the plan (A_1, A_2) we get the following graph.

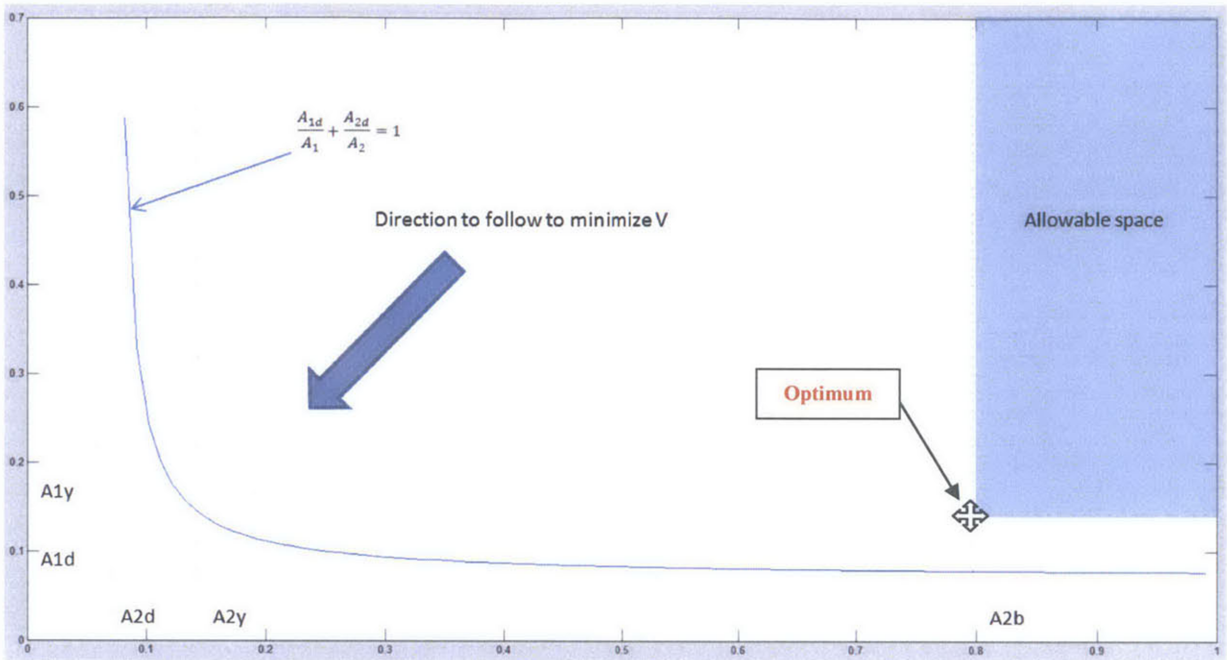

Figure 13: Allowable member areas for $\boldsymbol{\alpha}$ =360

The optimum for the problem is reached for $(A_1, A_2) = \left(A_{1y}, A_{2b}\right) = (0.1427cm^2, 0.7972cm^2)$ and the corresponding volume is $V_0^{(truss)} = 52.5427cm^3$.

In fact, increasing the requirement in terms of displacement constraints up to $\alpha = 500$ does not change the optimum in this configuration. This is mainly due to the small span of the beam.

3.2 Tensegrity optimization – No points added (n=0)

We are back to the same problem in terms of force applied and geometry except that we now allow the use of cables which have a higher strength but lower stiffness compared to the struts. Additionally, it is possible to prestress the system.

For a point to be in a prestressed state of equilibrium at least three members connecting to that node are needed or two collinear members pending there is a stabilizing support.

Here, the system is not prestressable. Indeed, the node where the force P is applied will move for any set of member forces different than $(0,0)$. That being said let us solve the problem without prestress. The only potential configuration is a cable for member 1 and a strut for member 2. Please note this configuration is actually stable if and only if the load is pointing down.

Since the system is internally isostatic, the member forces do not depend on the stiffness of the members. Hence, the expressions of the force in the members remain the same. Below is the new expression of the different area parameters following the same method as before.

For $i = 1,2$

$$A_{iy} = \frac{|F_i|}{f_{yi}}$$

$$A_{ib} = 2l_i\sqrt{\frac{\max(-F_i, 0)}{\pi E_i}}$$

$$A_{id} = \frac{l_i F_i^2}{PE_i u_d}$$

To the problem parameters previously used for the truss, we need to add the mechanical parameters for the cables. Let us assume $E_c = 17\,000kN.cm^{-2}$ and $f_{yc} = 100kN.cm^{-2}$.

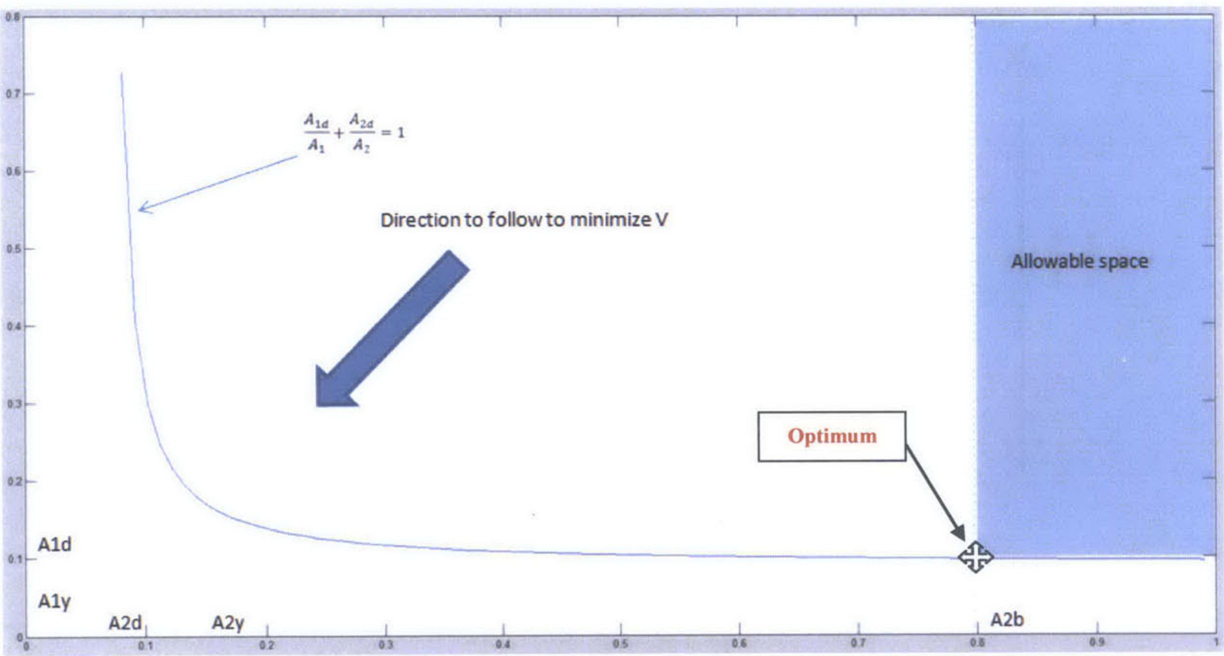

Figure 14 : Allowable member areas for $\boldsymbol{\alpha}$ =360

It is not clear on the graph above but the displacement constraint is governing for the cross-sectional area of member 1.

The optimum for the problem is reached for $(A_1, A_2) = \left(\frac{A_{1d}}{1-\frac{A_{2d}}{A_{2b}}}, A_{2b}\right) = (0.0976cm^2, 0.7972cm^2)$ and the corresponding volume is $V_0^{(tensegrity)} = 50.0190cm^3$.

Hence, the tensegrity configuration (even though it is not really stable for all loads) is a better choice than the corresponding truss configuration. Even though cables are softer than bars the additional strength helped reducing the volume by a small amount (-4.8%).

3.3 Truss optimization – One added point (n=1)

As another point is added, the complexity of the problem increases significantly.

There are now multiple feasible connectivities. The necessary condition for the truss to be stable is $2 * 4 - 4 \leq m$. The number of theses potential configurations to study is equal to:

$$\sum_{k=4}^{6} \binom{6}{k}$$

We get $15 + 6 + 1 = 22$ potential connectivity. If a member is used to connect the two supports, it won't contribute mechanically. All of the connectivity including this member can thus be disregarded. We now have only 6 configurations left. The one below plus all the configurations we get by removing one member only.

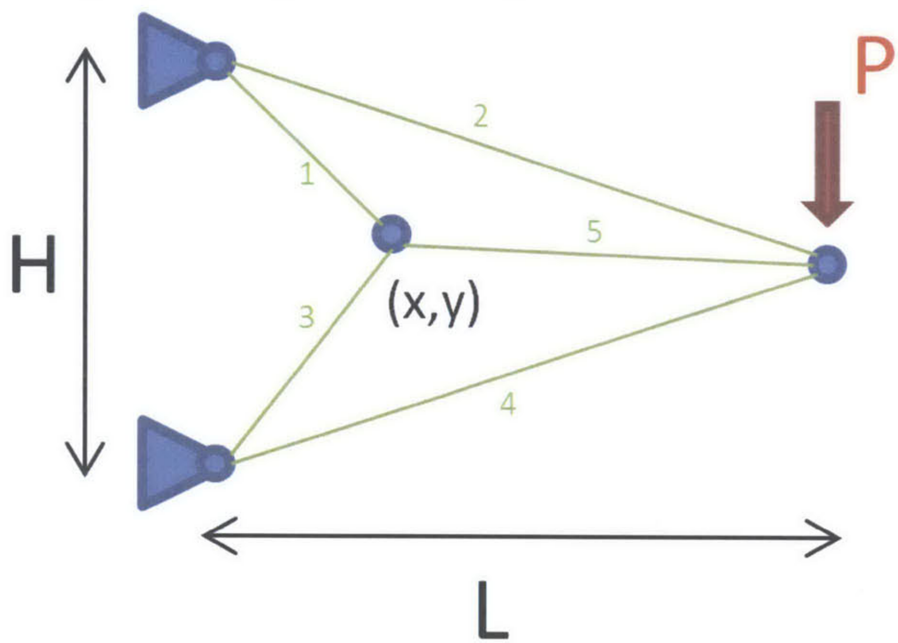

Figure 15 : Truss configuration n=1

The connectivity arrangements for which we remove member 1, 3 or 5 are disregarded as well. Indeed, the resulting structure will behave as the truss for n=0. No force is applied at the middle node so it does not contribute to the equilibrium of the system. Member superposition is not allowed.

Only two internally isostatic and one hyperstatic cases remain. Looking first at the internally isostatic cases (corresponding to the removal of member 2 or 4), it appears both buckling and yield constraints give a simple relationship like we have seen before in section 3.1 and 3.2 except that now the A_{ib} and A_{iy} depend on the geometric variables (x, y). This is true for any internally isostatic truss. Indeed, forces in the members depend only on the geometry. For the same reason, the A_{id} in the displacement constraint depend on (x,y) as well but, the relationship is more complicated. However, a necessary condition we can easily implement is $A_i > A_{id}$ for all i.

The function to optimize depends then only on the geometric variables (x,y):

$$\tilde{V}(x,y) := \sum_i l_i(x,y).\max\left(A_{id}(x,y); A_{ib}(x,y); A_{iy}(x,y)\right)$$

- Removing member 2

After exploring the (x,y) space (with a step size in both directions of 0.1cm) with the same data as before we get an optimum of $\tilde{V}_{min} = 48.3766cm^3$ for $(x,y) = (50,-11)$ and $(A_1, A_3, A_4, A_5) = (0.1573, 0.7109, 0, 0.1551)$.

Note that we only looked at the necessary condition for the displacement constraint. Checking a posteriori the displacement constraint with the optimum found we get:

$$\sum_i \frac{A_{id}}{A_i} = 0.7687 < 1$$

Note as well that in this configuration member 4 does not take any force and thus can have an area of 0. With the formulation of the problem in section 2, though, this member would have had an area of a_0 and maybe the optimum would have been changed.

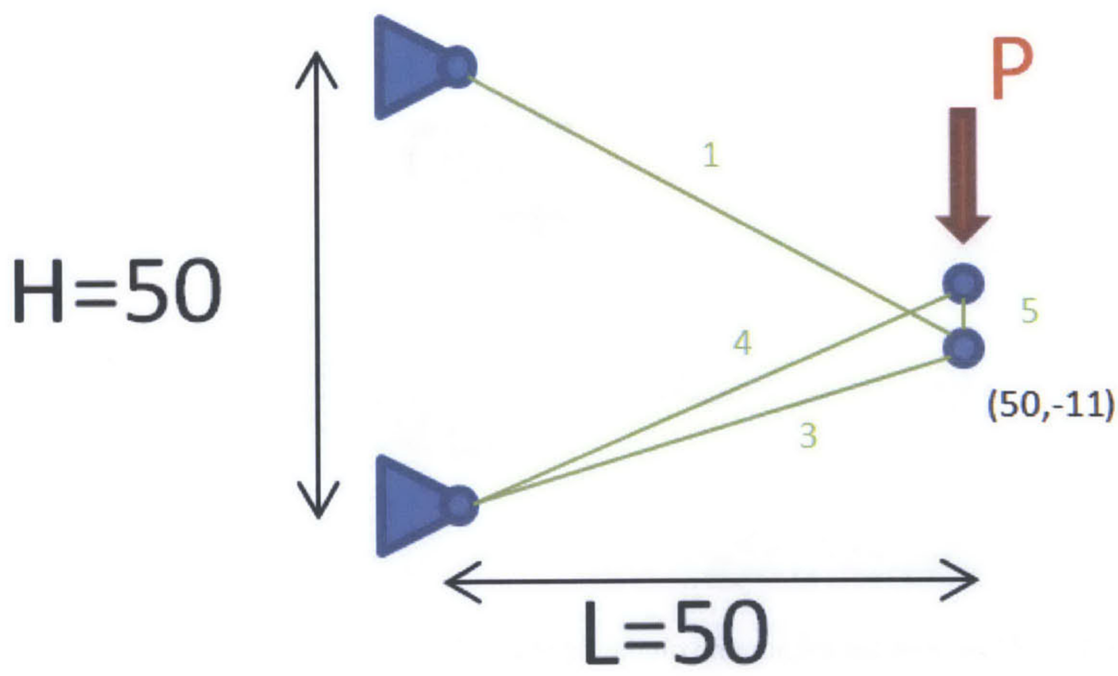

Figure 16 : One potential optimal configuration for truss problem n=1

Below, we have a plan and a 3D view of the minimum volume $\tilde{V}_{min}$ depending on the values of (x,y). The axis of member 4 acts like a barrier between two potential regions or valleys. We can interpret the top valley as the structure asking for the missing member 2 that provided suspension. The bottom valley can be seen as a way of reducing the buckling constraint on the bottom member. The transition between the two valleys occurs for $(x, y) = (50,0)$ which corresponds to the location of the tip node. For this degenerated configuration, we get the same results as for n=0 as the two nodes are rigidly linked.

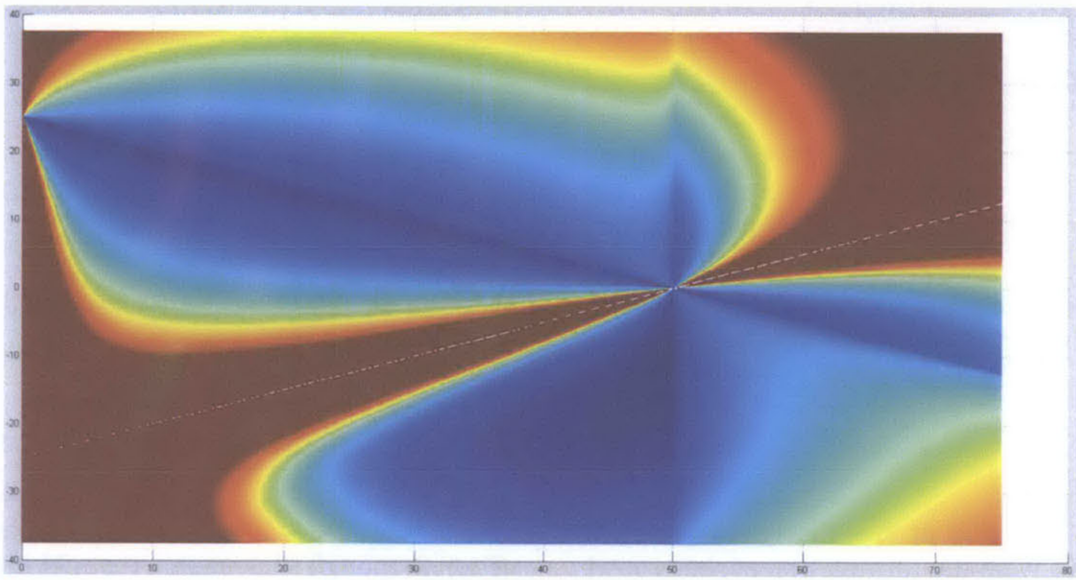

Figure 17 : Plan view of the minimum volume function $\tilde{V}_{min}$ – Truss n=1 – member 2 removed

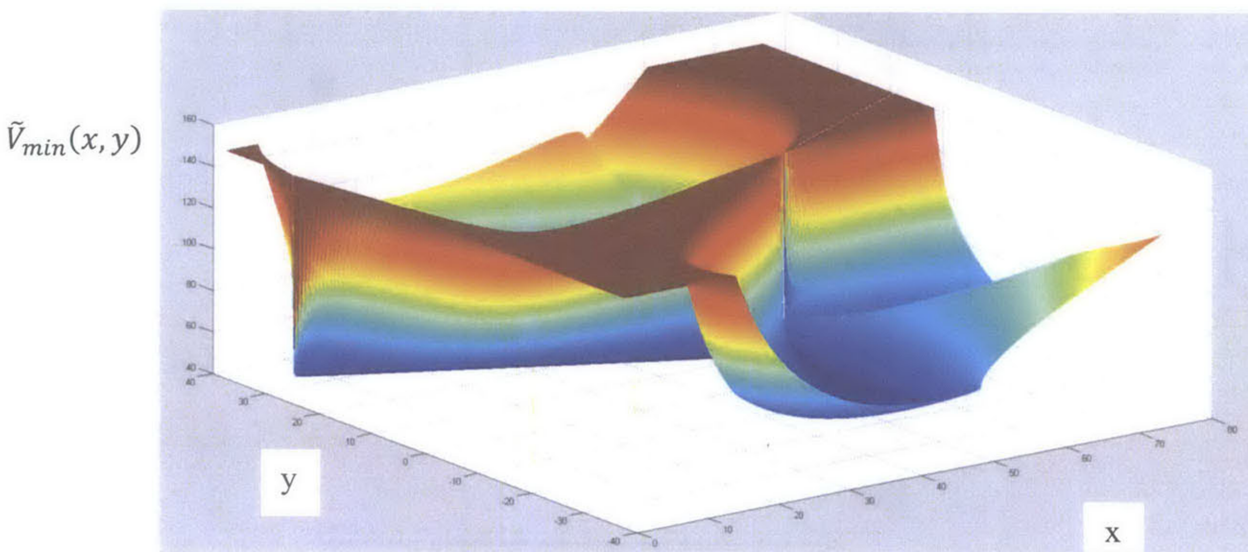

Figure 18 : 3D view of the minimum volume function $\tilde{V}_{min}$ - Truss n=1 – member 2 removed

Please note that the volume has been capped at $150cm^3$ in order to see the relevant part of the design space.

- Removing member 4

Following the same process, the optimum for this connectivity is $\tilde{V}_{min} = 30.1550cm^3$ reached for $(x, y) = (25.8, -13.8)$ and $(A_1, A_2, A_3, A_5) = (0.0151; 0.1334; 0.3961; 0.3897)$.

Checking a posteriori the displacement constraint with the optimum found we get:

$$\sum_i \frac{A_{id}}{A_i} = 0.6863 < 1$$

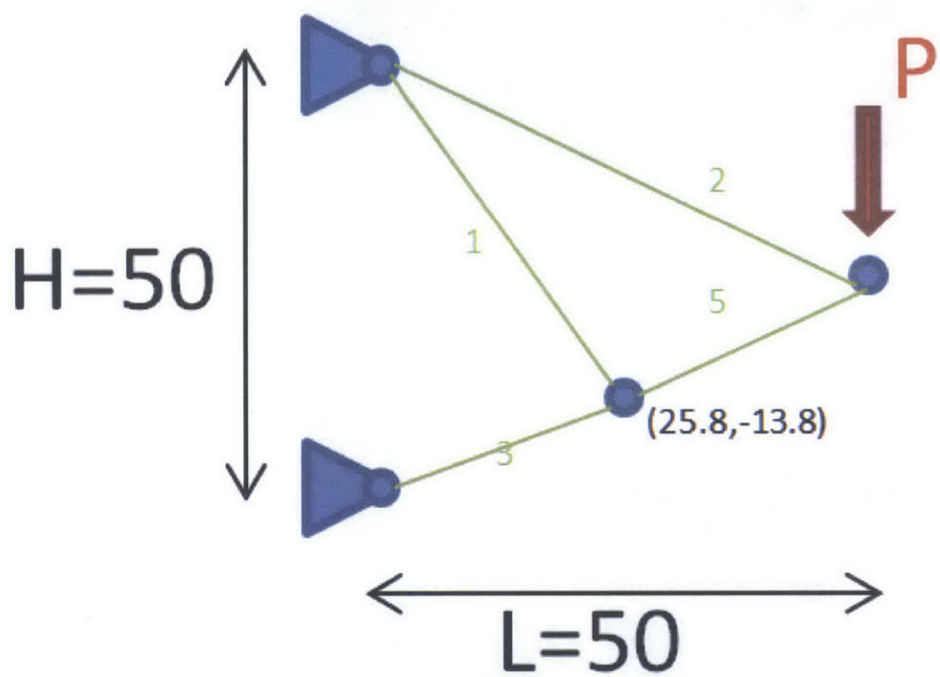

Figure 19 : Another potential optimal configuration for truss problem n=1

Looking at our optimum point we see that all members participate in the transfer of the force *P* to the supports. It is important to note the "moving" node is not located in the alignment of the removed member (For the abscissa 25.8 the corresponding point on member 4 would have been-12.1). It is edifying how the addition of a small member, namely 1, can increase significantly the performance of the structure compared to the truss optimization with n=0.

Similarly to what was found when removing member 2, on figure 18 and 19 below we have a barrier, where member 2 is, separating two valleys. The transition point between these two valleys is the location of the tip node.

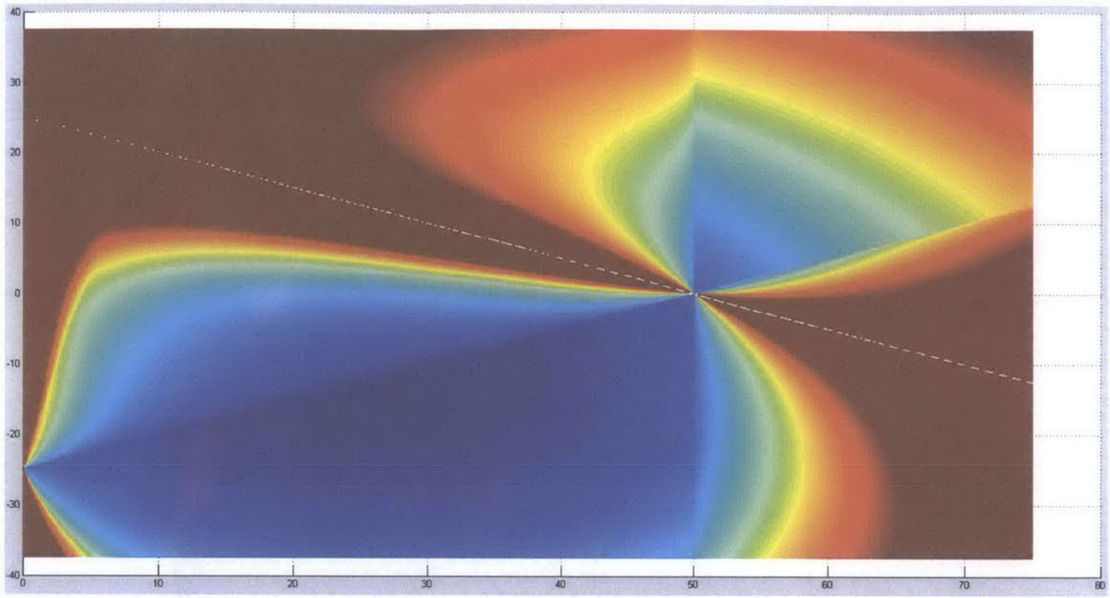

Figure 20 : Plan view of the minimum volume function $\tilde{V}_{min}$ – Truss n=1 – member 4 removed

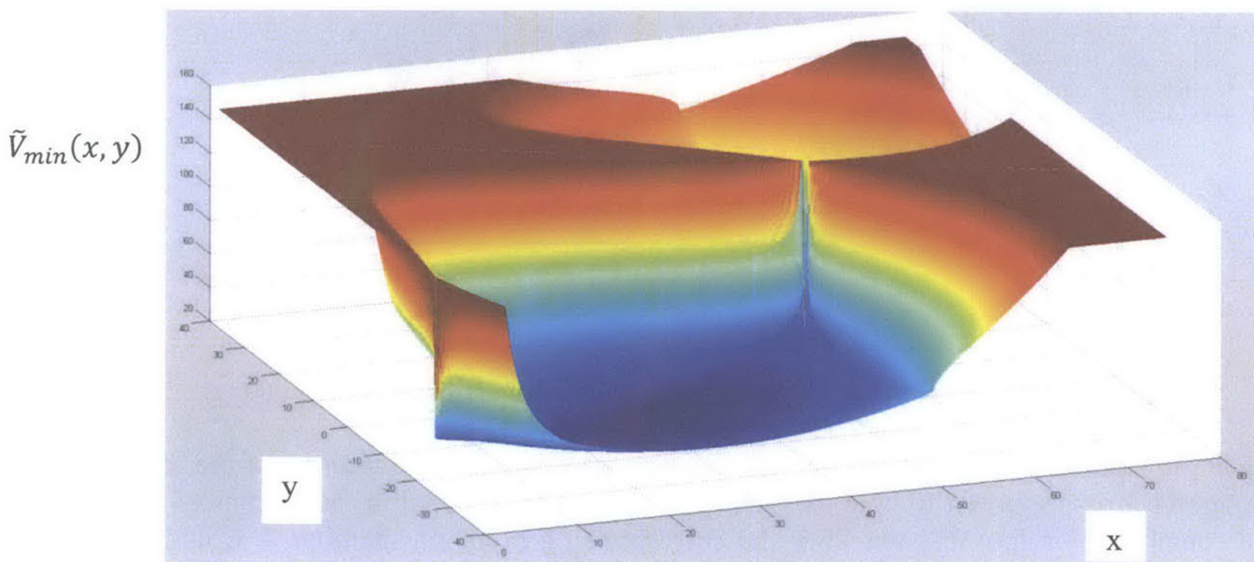

Figure 21 : 3D view of the minimum volume function $\tilde{V}_{min}$– Truss n=1 – member 4 removed

- Hyperstatic case

For this case all members are considered. Now, the complexity of the problem increases dramatically as the area parameters (A_{id}, A_{ib}, A_{iy}) depend on both the geometric variables and the cross-sectional area of all the members in the system. Hence, exploring the variables' space is no longer an option. To solve this problem, we explore the geometric variables' space with a step size of $0.1cm$ and call MATLAB's "*fmincon*" solver to find the optimal cross-sectional areas for the members for each pair of geometric variables. Setting the minimum area for a member a_0

to $0.01cm^2$, an optimum of $V_{min} = 46.0282$ is found for $(x, y) = (39.6, -13)$ and $(A_1, A_2, A_3, A_4, A_5) = (0.215; 0.0816; 0.5701; 0.01; 0.3897)$.

Here, the system wants member 4 gone. This is why the minimum allowable area is obtained for this element. Even if this is a small area, the forces in the system are changed drastically, and so do the required area, compared to the isostatic case with member 4 removed. The optimum volume is then higher.

The global optimum for a truss with $n = 1$ is thus the one found for the isostatic case with member 4 removed.

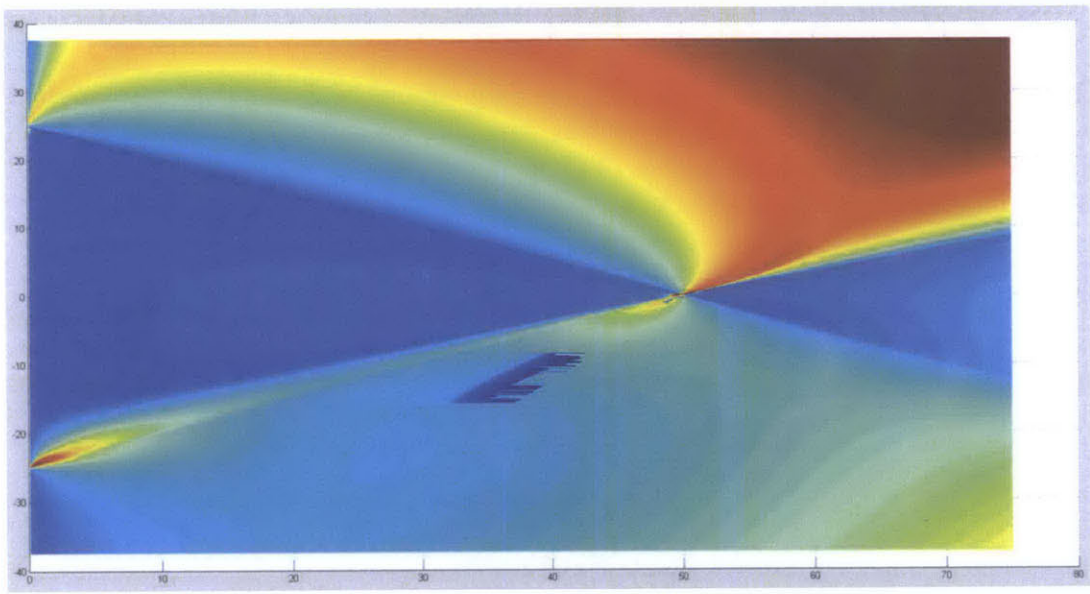

Figure 22 : Plan view of the minimum volume function V_{min} – Truss n=1 – hyperstatic case

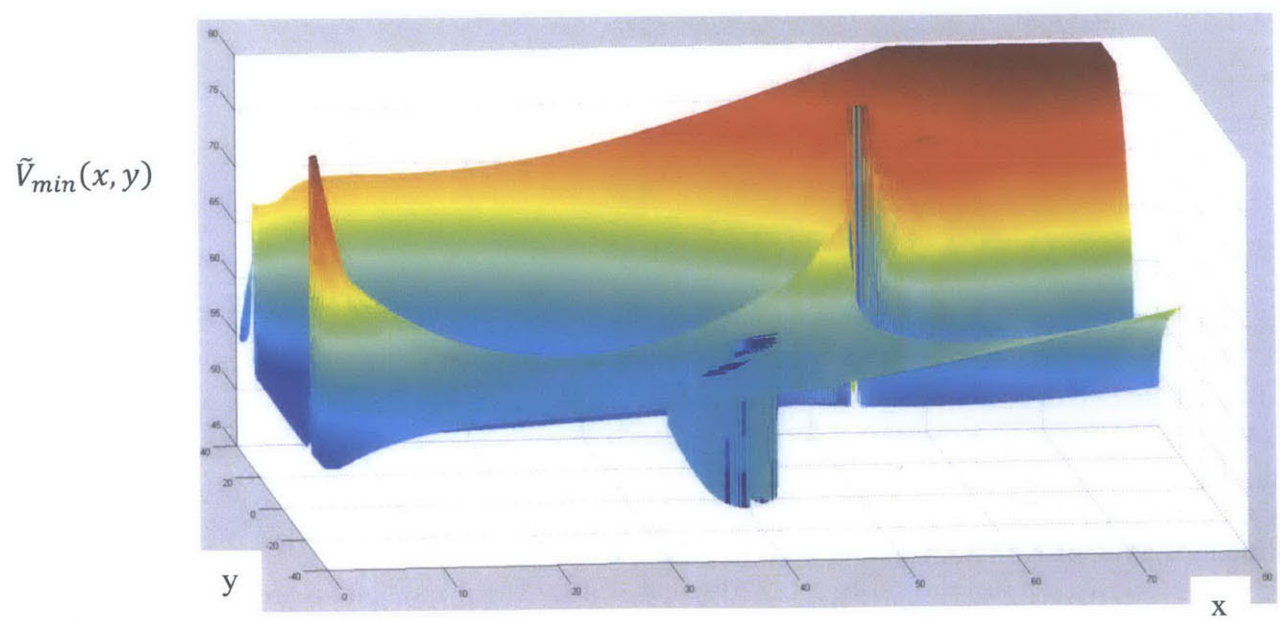

Figure 23 : 3D view of the minimum volume function V_{min}– Truss n=1 – hyperstatic case

Something to notice is the fact that the minimum volume function does not explode as quickly as in the isostatic cases when the added point is set in an awkward position for the structure. This is due to the redundancy in the system. In an isostatic structure there is only one load path whereas in a hyperstatic system there are several. Hence, if one path is not appropriate the load will find another way to the supports whereas in the isostatic case it is not possible. Additionally, it is interesting to see how a deep valley exists for $(x, y) \in [30{,}40]\ X\ [-20, -10]$. This could also be interpreted by redundancy in the structure. As the added point moves, a certain load path is activated. However, when the point reaches the valley, the corresponding geometry is particularly suitable for another load path which reveals itself to be more efficient.

3.4 Tensegrity optimization – One added point (n=1)

What was said in section 3.3 in terms of the configurations to be studied remains valid for tensegrity structures. Three connectivity cases must be considered. Looking at the nodes' equilibrium of the two isostatic cases, it is obvious that those systems are not prestressable. But we can still optimize their without prestress.

- Removing member 2

Let $(c_i, s_i)_{i=1,3..5}$ be the family of cosine and sine of the members' orientation in the plane. Since the system is isostatic, the forces in the elements can be determined by solving the nodes equilibrium.

$$F_4 = P\frac{c_5}{c_4 s_5 - c_5 s_4}$$

$$F_5 = -P\frac{c_4}{c_4 s_5 - c_5 s_4}$$

$$F_1 = F_5\frac{c_5 s_3 - c_3 s_5}{c_1 s_3 - c_3 s_1}$$

$$F_3 = F_5\frac{c_1 s_5 - c_5 s_1}{c_1 s_3 - c_3 s_1}$$

Depending on the location of the added point, the forces will change sign.

Since the system is soft, due to the presence of cables, the method that consists in looking at the value of $\tilde{V}_{min}$ depending on the value of (x, y) does not work anymore. Indeed, the minimum found with this method does not meet the displacement criterion ($\sum_i \frac{A_{id}}{A_i} = 1.1857 > 1$).

The optimum in terms of the cross-sectional area of the members can still be found (see section 3.5). By exploring the variables space with a step size of 0.1cm in the x direction and 0.1cm in the y direction, an approximation of the optimum is found: $V_{min} = 47.1940cm^3$ for $(x, y) = (50, -9.9)$ and $(A_1, A_3, A_4, A_5) = (0.1405; 0.7200; 0; 0.1036)$. Members 3 and 5 are bars while 1 is a cable.

It is the same type of minimum (the added point is located about $10cm$ below the load application point) than the one found for the truss system except that we have a small decrease in volume (-2.4%) thanks to the extra strength of the cable.

- Removing member 4

The expressions of the forces in the members have the same form as before except that (c_4, s_4) is replaced by (c_2, s_2). Following the same method, an optimum of $V_{min} = 28.2578cm^3$ is reached for $(x, y) = (25.8, -13.5)$ and $(A_1, A_3, A_2, A_5) = (0.0096, 0.3986, 0.1034, 0.3888)$. Members 1 and 2 are cables while member 3 and 5 are bars.

Again, we have a solution which is very similar to the one obtained for a truss but slightly better in terms of volume (-6.3%).

- Hyperstatic case

This is definitely the case with more richness so far. Indeed, this system is now prestressable. In order to enforce an auto-equilibrated prestress force field, only one prestress force variable is needed as the system is one time hyperstatic. Let $\boldsymbol{F}_{0,5}$ be that variable. It lives in $[-f_{y,b}A_5, f_{y,c}A_5]$. The other prestress forces in the members are:

$$\boldsymbol{F}_{0,1} = \boldsymbol{F}_{0,5}\frac{c_5 s_2 - c_2 s_5}{c_1 s_2 - c_2 s_1}$$

$$\boldsymbol{F}_{0,2} = \boldsymbol{F}_{0,5}\frac{c_1 s_5 - c_5 s_1}{c_1 s_2 - c_2 s_1}$$

$$\boldsymbol{F}_{0,3} = -\boldsymbol{F}_{0,5}\frac{c_5 s_4 - c_4 s_5}{c_3 s_4 - c_4 s_3}$$

$$\boldsymbol{F}_{0,4} = -\boldsymbol{F}_{0,5}\frac{c_3 s_5 - c_5 s_3}{c_3 s_4 - c_4 s_3}$$

To solve the system, the function "*fmincon*" is called in MATLAB. Starting with a prestress of $\boldsymbol{F}_{0,5} = 1kN$ with the corresponding connectivity due to the unilateral behavior of members and ranging only on the positive side $[0, f_{y,c}A_5]$ result in a local minimum that has a larger volume compared to the previous cases (about $55cm^3$). The mirror configurations with a starting prestress force in member 5 of $\boldsymbol{F}_{0,5} = -1kN$ and looking only the negative range $[-f_{y,b}A_5, 0]$, gives an optimum of about $65cm^3$.

It appears here that the prestress in the system does not help saving materials.

3.5 Specific derivation for isostatic systems

The case of isostatic structures, in the particular cantilever situation, is simple enough so that we can derive analytically the optimum cross-sectional areas for a fixed geometry. Indeed, the forces in the members depend only on the geometric variables; so do the quantities (A_{id}, A_{ib}, A_{iy}). Additionally, an isostatic tensegrity system is not prestressable. Besides, for a fixed geometry the sign of the forces in the members is defined so there is only one choice possible in terms of cables/bars.

Looking at section 3.1 and 3.2 will help understand how the area optimum is found. Let $n \in \mathbb{N}$ be the number of added points to the problem and $(x_i, y_i)_{i=1..n}$ be the coordinates of these added points. Assume $A_{id}((x_i, y_i)_{i=1..n}) > 0$ for all i. Consider the following scenarios:

- Displacement constraint only

The optimal areas for the members are on the frontier defined by the curve:

$$\sum_{i=1}^{m} \frac{A_{id}}{A_i} = 1$$

Picking one area variable, say the one corresponding to index m without any loss in generality (a reindex could be performed), one can enforce the frontier condition by expressing it in terms of the other variables:

$$A_m = \frac{A_{md}}{1 - \sum_{i=1}^{m-1} \frac{A_{id}}{A_i}}$$

The volume function is now a function of $m-1$ variables:

$$V((A_i)_{i=1..m-1}) = \sum_{i=1}^{m-1} l_i A_i + l_m \frac{A_{md}}{1 - \sum_{i=1}^{m-1} \frac{A_{id}}{A_i}}$$

It is a strictly convex function and goes to infinity if one of the A_i tends to A_{id} or $+\infty$. A unique minimum thus exists and is found by annulling the gradient. For $j \in [\![1, m-1]\!]$ the partial derivative corresponding to A_j is:

$$\frac{\partial V}{\partial A_j} = l_j - l_m \frac{A_{md} A_{jd}}{A_{jd}^2 \left(1 - \sum_{i=1}^{m-1} \frac{A_{id}}{A_i}\right)^2}$$

Setting this equal to zero, we get:

$$\sum_{\substack{i=1 \\ i \neq j}}^{m-1} \frac{A_{id}}{A_i} + \left(A_{jd} + \sqrt{\frac{l_m A_{md} A_{jd}}{l_j}}\right) \frac{1}{A_j} = 1$$

Where we have kept the positive root of the square equation as the displacement constraint imposes $1-\sum_{i=1}^{m-1}\frac{A_{id}}{A_i}>0$.

Rewriting the equations corresponding to the nullity of the $m-1$ partial derivatives in a compact matrix form, the following system is obtained:

$$\boldsymbol{T}\begin{pmatrix}\frac{1}{A_1}\\ \vdots \\ \frac{1}{A_{m-1}}\end{pmatrix}=\begin{pmatrix}1\\ \vdots \\ 1\end{pmatrix}$$

Where $\boldsymbol{T}$ is the $(m-1)\ X\ (m-1)$ matrix whose general term is:

$$(\boldsymbol{T})_{ij}=\begin{cases}A_{dj} & for\ i\neq j\\ A_{jd}+\sqrt{\dfrac{l_m A_{md} A_{jd}}{l_j}} & for\ i=j\end{cases}$$

The determinant of the matrix $\boldsymbol{T}$ can be calculated (see Appendix 3) and is equal to:

$$\prod_{i=1}^{m-1}\sqrt{\frac{l_m A_{md} A_{id}}{l_i}}+\sum_{i=1}^{m-1}A_{id}\prod_{\substack{j=1\\ j\neq i}}^{m-1}\sqrt{\frac{l_m A_{md} A_{jd}}{l_j}}$$

Considering all the members in this expression are strictly positive the system is invertible and the optimum areas for the members, that we will call(A_{ik}), are found by inverting the system. Note that A_{mk} is obtained with the formula $A_{mk}=\frac{A_{md}}{1-\sum_{i=1}^{m-1}\frac{A_{id}}{A_{ik}}}$.

In some degenerate cases, $A_{id}((x_i,y_i)_{i=1..n})=0$ for certain values of i. This happens when a member does not pick any load due to its orientation (see for instance 3.3 when member 2 is removed). In these particular cases, the member does not contribute at all to the mechanical equilibrium of the system but still has to be there to maintain stability. A minimum area can be affected to it; it will just offset the value of the volume function. The reasoning above still applies but the indexes corresponding to the null A_{id} are not considered in the sum defining the displacement constraint curve.

- All the constraints considered

Buckling and yielding constraints are now taken into account.

If $A_{ik}((x_i,y_i)_{i=1..n})\leq\max\left(A_{ib}((x_i,y_i)_{i=1..n});A_{iy}((x_i,y_i)_{i=1..n})\right)$ for all i then the optimal area for the members is $A_i^{(opt)}=\max\left(A_{ib}((x_i,y_i)_{i=1..n});A_{iy}((x_i,y_i)_{i=1..n})\right)$.

If for some $A_{ik}((x_i, y_i)_{i=1..n}) > max\left(A_{ib}((x_i, y_i)_{i=1..n}); A_{iy}((x_i, y_i)_{i=1..n})\right)$, the optimum is changed. Let us partition $[\![1, m]\!] = I \cup J$, where I is the collection of indexes for which $A_{ik}((x_i, y_i)_{i=1..n}) > max\left(A_{ib}((x_i, y_i)_{i=1..n}); A_{iy}((x_i, y_i)_{i=1..n})\right)$ while J is the one for which $A_{ik}((x_i, y_i)_{i=1..n}) \leq max\left(A_{ib}((x_i, y_i)_{i=1..n}); A_{iy}((x_i, y_i)_{i=1..n})\right)$. Cases where some members do not take forces are not considered (see remark above).

The optimum is then found by taking the minimum allowable area for all the members of indexes in J and finding the optimum volume on the reduced displacement constraint curve. The matrix $\boldsymbol{T}$ is then smaller and the system to solve to get the optimum values of $\left(A_j\right)_{j\in J}$ is:

$$\boldsymbol{T}\begin{pmatrix} \frac{1}{A_1} \\ \vdots \\ \frac{1}{A_{\#J-1}} \end{pmatrix} = \begin{pmatrix} 1 - \sum_{i\in I} \frac{A_{id}}{max\left(A_{ib}((x_i, y_i)_{i=1..n}); A_{iy}((x_i, y_i)_{i=1..n})\right)} \\ \vdots \\ 1 - \sum_{i\in I} \frac{A_{id}}{max\left(A_{ib}((x_i, y_i)_{i=1..n}); A_{iy}((x_i, y_i)_{i=1..n})\right)} \end{pmatrix}$$

Note that the derivation above accounted for only one displacement constraint.

4. Computational approach to solve the general problem

4.1 Characteristics of the problem and approach

The optimization problem has been well-formulation in section 2 and we know a global minimum exists. Finding it is the most difficult part though. Our case in particular is very complex. Indeed the problem is non-convex and nonlinear and it includes both continuous and integer variables (mixed-integer). Nowadays, numerical optimization works best for convex nonlinear problem and some simple mixed-integer formulations.

4.1.1 Choosing the starting points

To non-convexity in itself will not cause any computational issue. The standard algorithm will just converge to a local minimum which is the closest to the starting point which was provided to it. It is then necessary to have a strategy to choose the starting points wisely.

- Connectivity

In order not to favor any particular path, the starting connectivity will be maximum, i.e. all the points are connected to all the points they can be connected to. For a tensegrity, there is no specific rule for the partitioning between struts and cables for the start point.

- Geometric variables

Looking at the volume function plots in section 3, it seems that different valleys are delimited by existing members. Hence, if we have solved the problem for $n = k - 1$, good starting points for the $n = k$ problem could be obtained by choosing the previously found set of points and locating the added point between the existing members. The algorithm could then be launched several times with different starting points and the best solution will be kept in the end.

- Cross-sectional area variables

In order not to favor any load path by making a member bigger than the others, the starting point for the cross-sectional area variables gives the same area to every member. Potentially, a good alternative could be to choose the starting areas such that all the members have the same axial rigidity. This assumes the geometry has been defined.

- Prestress forces variables

The equality constraint which is used to enforce the prestress equilibrium is verified if the system is not prestress. Hence, in order for the algorithm to be able to explore prestressed systems, a good starting point for the prestress forces variables could be a random set of forces or if the geometry is provided an auto-equilibrated field of forces.

4.1.2 Programming approach

Since no existing typical optimization algorithm can solve the general problem as a whole, the idea behind the computing approach was to divide the optimization into two parts. A global genetic algorithm is dealing with the geometric and connectivity variables while a standard optimization sub-algorithm (SQP) takes care of the prestress and cross sectional area variables under the given constraint.

Below is a short description on how the two algorithms work.

4.2 Description of the algorithms

4.2.1 Genetic algorithm (GA)

A genetic algorithm, as its name points out, is an algorithm that mimics the natural section process. Starting with a given population the best individuals are kept while the others are subjected to mutations and reproduction (or crossover). An individual is a set of values for the variables and how good they perform depends on the values of the objective function and the constraints obtained with them. If constraints are not satisfied a penalty is applied. A new round starts with the next generation and the algorithm stops when a whole population is sufficiently alike such that no mutations would make the situation better.

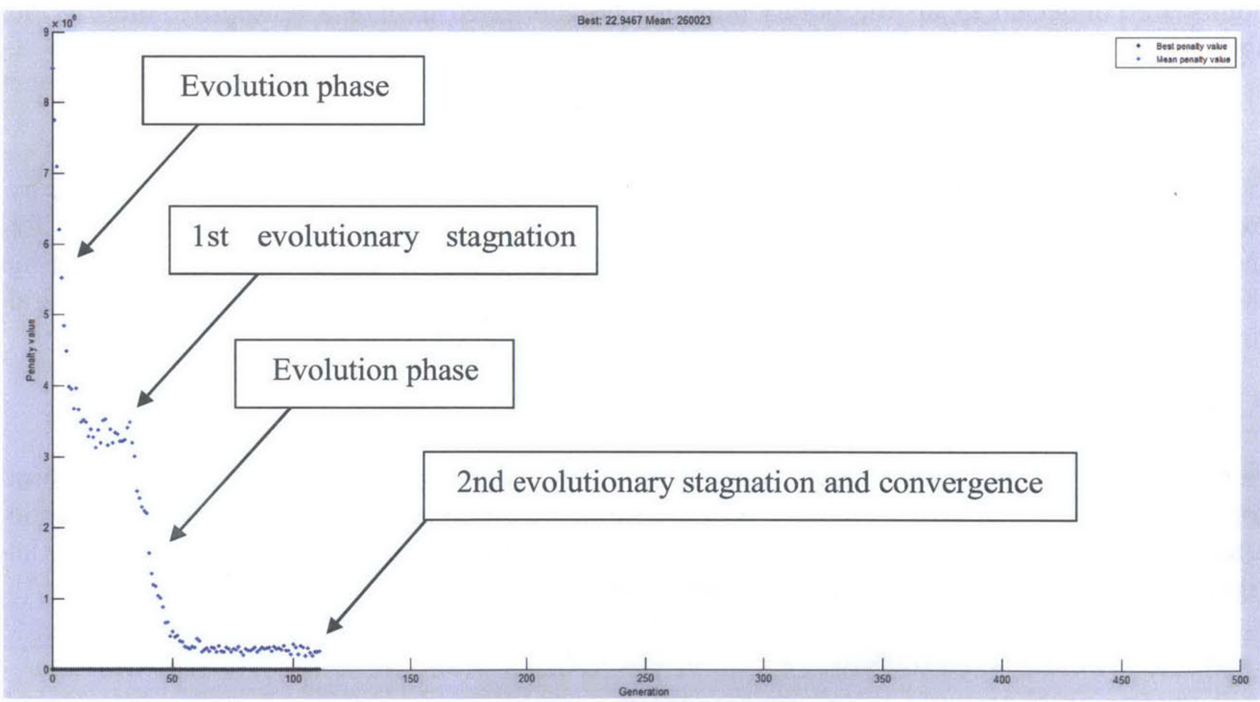

Figure 24 : Evolution of the penalty value over the generations until convergence

It is interesting to see on this Figure 24 how the optimum is found. Evolution phases characterized by a tremendous decrease in the penalty value are followed by evolutionary stagnant phases where the penalty value does not change much. A biology analogy to this process could be the following: A profitable mutation in an individual causes him to be selected and be highly involved in the reproduction process. The evolution phase is then due to the multiple crossovers that increase the efficiency of the mutation to its maximum. Another evolutionary stagnant phase follows.

This type of algorithm is metaheuristic, meaning that it relies on a probabilistic sampling and evaluation. There is no proof to show the convergence but it has been evidenced that on problems where the solution is known by classical programming, a GA would give the same answer.

One of the main advantages of this method though is that it can deal with very complex optimization, including mixed-integer programming and can manage the lack of regularity of the objective function and or, the constraints. Additionally, when a typical optimization algorithm will find the local minimum which is the closest to the starting point, a GA, pending it is correctly parameterized, will have more chances of finding the global optimum.

4.2.2 Sequential Quadratic Programming (SQP)

This algorithm represents the state of the art in terms of classical constrained nonlinear programming. It can be seen as the application of a quasi-Newton scheme but on a constrained problem. It relies on the decomposition of the main nonlinear problem in quadratic subproblems, for which the solving method is well known and efficient. At each step an approximation of the Lagrangian function hessian matrix is computed.

This method is known to be very efficient but cannot deal with mixed-integer formulation or low-regularity (as the hessian matrix is calculated) problems.

4.3 Results

Below are the results obtained for both truss and tensegrity by using this computing approach:

n	Truss	Tensegrity
0	$V = 52.4137cm^3$	$V = 49.6271cm^3$
	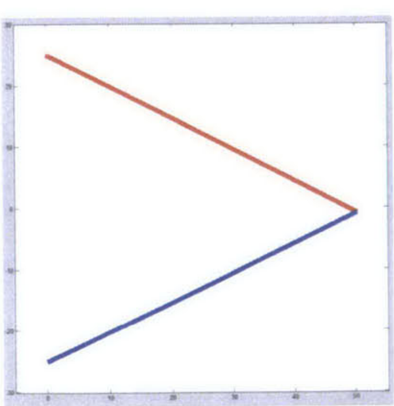	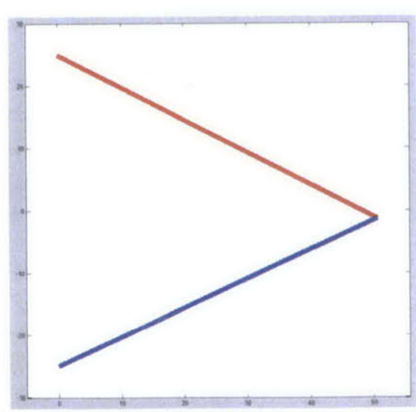

n	Truss	Tensegrity
1	$V = 30.1195cm^3$	$V = 28.9045cm^3$
	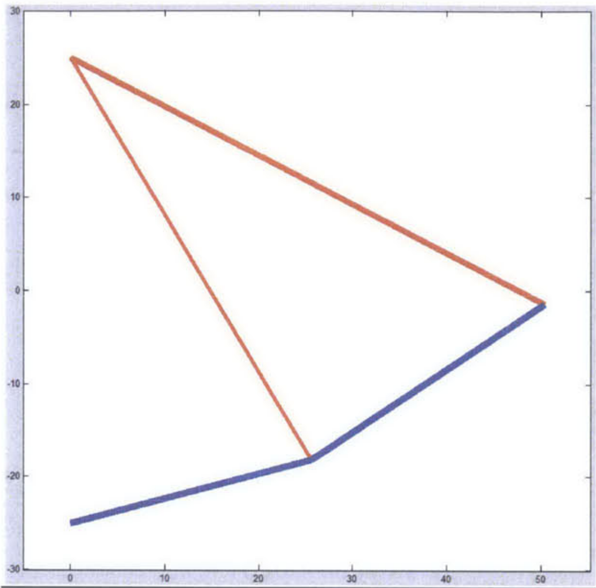	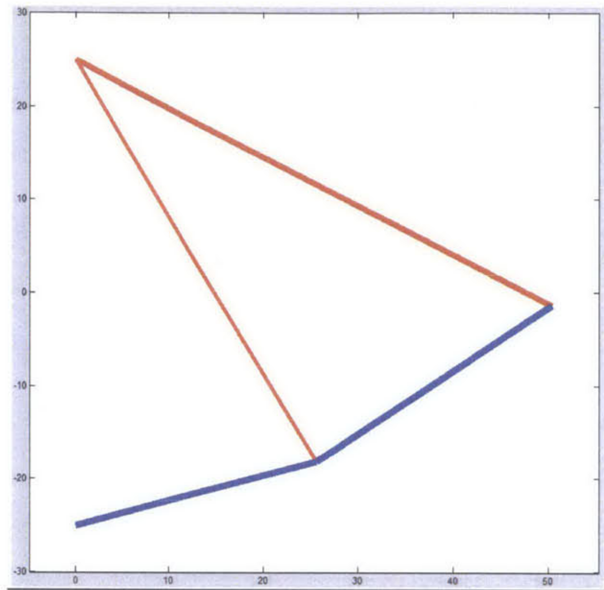
2	$V = 23.3193cm^3$	***ABNORMAL*** - $V = 4cm^3$
	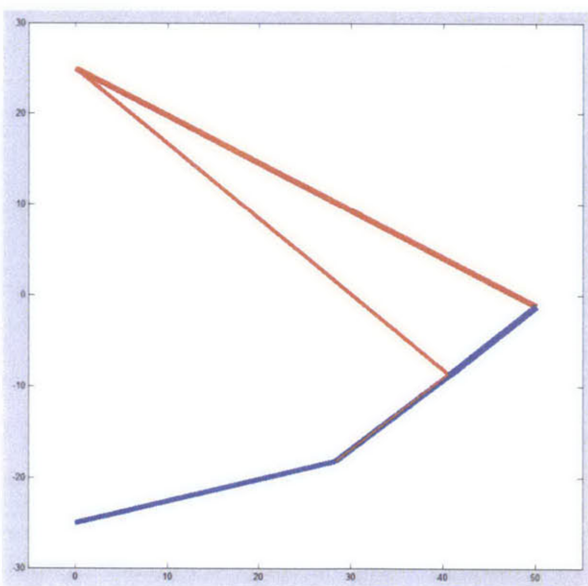	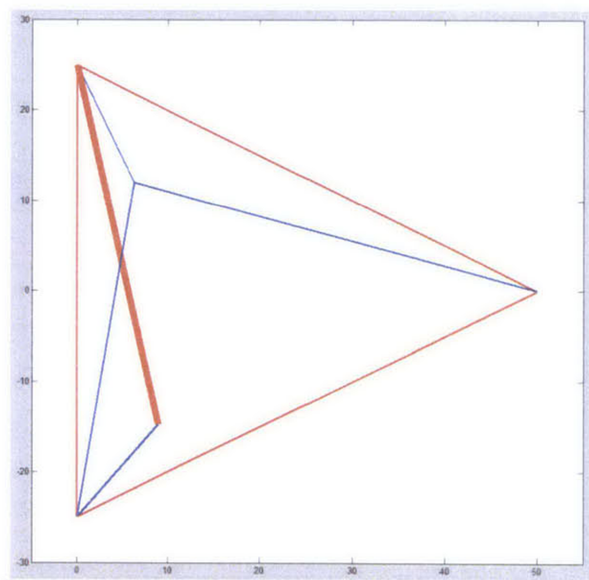

n	Truss	Tensegrity
3	$V = 22.9467cm^3$	$V = --\ cm^3$
	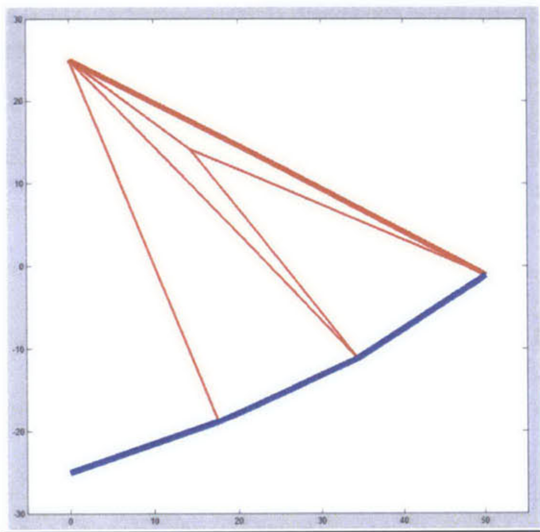	*Not computed*
4	$V = 20.3900cm^3$	$V = --\ cm^3$
	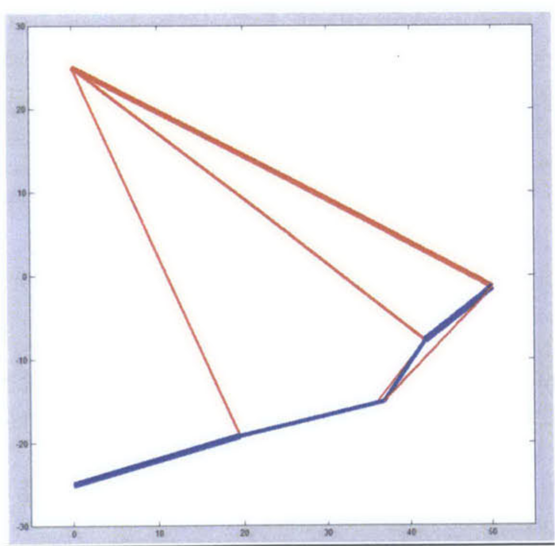	*Not computed*

Table 3 Results from the numerical optimization

Note that in the plots above, red represents tension while blue is compression. For tensegrities, red and blue also identifies cables and struts respectively. Only the volumes of the configurations are given for clarity.

The results obtained for the cases $n = 0$ and $n = 1$ with both tensegrities and trusses are coherent with the values found in section 3 (slight differences are due to the algorithm tolerances). However, for greater values of added points n, the geometries obtained could be questionable. For trusses, $n = 2$ or $n = 4$, some members are aligned/superimposed on each other for instance.

Globally, it seems that the volume is decreasing as we add points to the problem and that tensegrity configurations are slightly lighter compare to their associated truss configurations. It does not seem to be due to the prestress feature of tensegrities but more about the extra strength of cables.

For this particular problem, material savings are realized mainly by splitting the long compressive member at the bottom into several ones suspended with tension members to the top.

4.4 Remarks

The algorithm obtained is somewhat performing but there is definitely room for improvement in its implementation. It is very long to run and results sometimes do not make sense. It is important to remember that when the results do make sense, the configuration obtained represents only a local minimum. The GA will tend to give a global solution but the SQP converges towards the closest minimum due to the non-convexity of the problem.

The viability of this computing approach relies on the choice of various parameters. One of them that has shown to be a key parameter, is the limiting value on the conditioning of the extracted stiffness matrix associated with the non-fixed degrees of freedom $\boldsymbol{K_{MM}}$. An ill-conditioned matrix will tend to be sensitive to perturbations if it is used to invert a system. Results could potentially be wrong if a poor geometry causes $\boldsymbol{K_{MM}}$ to be ill-conditioned. This is what happened with the tensegrity configuration for $n = 2$. Currently, the conditioning of $\boldsymbol{K_{MM}}$ was measured calling MATLAB's function *rcond*, which returns the absolute value of the ratio of the smallest eigenvalue to the highest one. A well-conditioned matrix will have a *rcond* ratio close to 1 while a badly-scaled matrix will have a ratio close to 0. In the program, a configuration for which matrix $\boldsymbol{K_{MM}}$ was poorly scaled, $rcond(\boldsymbol{K_{MM}}) < 10^{-5}$ was the criterion applied, was rejected right away without computing the constraints. Subsequently, a big penalty was applied for the volume of these configurations.

Other key parameters to be selected with care include the genetic algorithm parameters. The size of the population, the number of generations and the mutation and cross-over rates to consider are crucial items for an efficient convergence of the GA. Too small mutation and cross-over rates will cause the algorithm to stagnate on the initial population while if they are too high the algorithm will give random populations at each round.

It is thus important to keep a critical eye when analyzing the results obtained.

Conclusion and perspectives

The approach presented in this document seems to be very fertile but in many ways it is perfectible. Some reliable results (small values of n) were obtained and then confirmed with the numerical optimization method that was designed. However, when the complexity of the problem increases, more added points or more constraints, the performance of the numerical optimization is uncertain. It depends on a lot of parameters and a fine-tuning will have to be performed, in accordance with the problem considered, to ensure reliability.

Two main suggestions can be made as a result of this study. First, it seems the sequence (V_n) of minimal volumes depending on the number of added points tends to be decreasing with n for the cantilever problem. It is consistent with the idea that we are approaching a solid beam with articulated structures. Further investigation will have to be carried to determine the true nature of this sequence. A key question to be answered would be to know if it keeps on decreasing or if it reaches a minimum for a specific value n_0.

The second suggestion is that tensegrity systems do not seem to decrease significantly the mass of a structure compared to regular truss systems. The reduction that was observed is due to the fact that cables have a higher yield stress compared to regular S235 steel. Prestress does not seem to help decreasing the mass of the system in tensegrities as most of the optimal solutions for tensegrities were isostatic, and then not prestressable. Nevertheless, even if tensegrity do not particularly help in terms of material savings, they still have some interesting properties like deployability and more research should go into this field of study.

In terms of perspectives to pursue further this research, one could refine the numerical method described previously and especially fine-tune the key parameters. It would be interesting to solve the problem for larger values of n and for different optimization problems than the cantilever situation and add consider more constraints.

Bibliography

Ingber, D. E. (2003). Tensegrity I. Cell structure and hierarchical systems biology. *Journal of Cell Science* , 116: 1157-1173.

Jarre, F., Kocvara, M., & Zowe, J. (1998). OPTIMAL TRUSS DESIGN BY INTERIOR-POINT METHODS. *SIAM J. OPTIM.* , Vol. 8, No. 4, pp. 1084-1107.

Lalvani, H. (1996). Origins of tensegrity: views of Emmerich, Fuller and Snelson. *International Journal of Space Structures* , 11:27-55.

Latteur, P. (2006). Chapitre 13. Les câbles. Dans P. Latteur, *Calculer une structure – De la théorie à l'exemple* (p. 488 pages). Academia-Bruylant.

Michell, A. G. (1904). The limit of economy in frame structures. *Philosophical Magazine* , 8:589-597.

Motro, R., & Vassart, N. (2001). 10. Tensegrity Systems. Dans VA, *Deployable structures.* S. Pellegrino.

Rhode-Barbarigos, L., Schulin, C., Bel Hadj Ali, N., Motro, R., & Smith, I. (2012). Mechanism-based approach for the deployment of a tensegrity-ring module. *Journal of Structural Engineering 138* , 4: 539-548.

Skelton, R. E., & de Oliveira, M. C. (2009). *Tensegrity Systems.* San Diego: Springer.

Appendices

Appendix 1 - Derivation of the static equilibrium equation with the stiffness method

Notation precision: In the following, I note $(\boldsymbol{E}_{ij}^{nm})$ the canonical basis of $M_{n,m}(\mathbb{R})$ and $\boldsymbol{I}^{nn}$ the identity matrix of $M_n(\mathbb{R})$. Matrices and vectors are bolded.

A.1.1 Member stiffness matrix

The stiffness matrix for a member of start point A and end point B is defined as the matrix $\boldsymbol{k}$ such that:

$$\begin{pmatrix} \boldsymbol{F}_A \\ \boldsymbol{F}_B \end{pmatrix} = \boldsymbol{k} \begin{pmatrix} \boldsymbol{U}_A \\ \boldsymbol{U}_B \end{pmatrix}$$

Where $(\boldsymbol{F}_A, \boldsymbol{U}_A)$ and $(\boldsymbol{F}_B, \boldsymbol{U}_B)$ are the pair forces applied and displacement at node A, B respectively. $\boldsymbol{k}$ can be decomposed in the following manner:

$$\boldsymbol{k} = \begin{pmatrix} \boldsymbol{k}_{AA} & \boldsymbol{k}_{AB} \\ \boldsymbol{k}_{BA} & \boldsymbol{k}_{BB} \end{pmatrix}, \text{ with } \boldsymbol{k}_{AA} = \boldsymbol{k}_{BB} = -\boldsymbol{k}_{AB} = -\boldsymbol{k}_{BA}$$

In a Cartesian coordinate system, we have:

$$\boldsymbol{k}_{AA} = \frac{EA}{l} \begin{pmatrix} \cos^2\alpha * \cos^2\gamma & \sin\alpha * \cos\alpha * \cos^2\gamma & \cos\alpha * \cos\gamma * \sin\gamma \\ \sin\alpha * \cos\alpha * \cos^2\gamma & \sin^2\alpha * \cos^2\gamma & \sin\alpha * \cos\gamma * \sin\gamma \\ \cos\alpha * \cos\gamma * \sin\gamma & \sin\alpha * \cos\gamma * \sin\gamma & \sin^2\gamma \end{pmatrix}, \text{ in 3D}$$

Or

$$\boldsymbol{k}_{AA} = \frac{EA}{l} \begin{pmatrix} \cos^2\alpha & \sin\alpha * \cos\alpha \\ \sin\alpha * \cos\alpha & \sin^2\alpha \end{pmatrix}, \text{ in 2D}$$

Where E is the young's modulus of the material the member is made of, A is the resisting cross-sectional of the member and l is its rest length, α is the longitude angle and γ is the latitude angle.

A.1.2 Assembling the system stiffness matrix

With the variables introduced in section 2.1, let us derive the characteristic stiffness matrix ${\boldsymbol{k}_{AA}}^{(h)}$ for member h.

The product $\boldsymbol{B}_{ih} := \boldsymbol{l}^{-1}\boldsymbol{C}^{(h)}\boldsymbol{N}\boldsymbol{E}_{ih}^{3m}$, returns a diagonal matrix with only one non-zero coefficient on the diagonal at place (h, h):

In 3D:

- $\boldsymbol{B}_{1h} = \boldsymbol{l}^{-1}\boldsymbol{C}^{(h)}\boldsymbol{N}\boldsymbol{E}_{1h}^{3m} = \cos\alpha * \cos\gamma\, \boldsymbol{E}_{hh}^{mm}$
- $\boldsymbol{B}_{2h} = \boldsymbol{l}^{-1}\boldsymbol{C}^{(h)}\boldsymbol{N}\boldsymbol{E}_{2h}^{3m} = \sin\alpha * \cos\gamma\, \boldsymbol{E}_{hh}^{mm}$
- $\boldsymbol{B}_{3h} = \boldsymbol{l}^{-1}\boldsymbol{C}^{(h)}\boldsymbol{N}\boldsymbol{E}_{3h}^{3m} = \sin\gamma\, \boldsymbol{E}_{hh}^{mm}$

In 2D:

- $\boldsymbol{B}_{1h} = \boldsymbol{l}^{-1}\boldsymbol{C}^{(h)}\boldsymbol{N}\boldsymbol{E}_{1h}^{2m} = \cos\alpha\, \boldsymbol{E}_{hh}^{mm}$
- $\boldsymbol{B}_{2h} = \boldsymbol{l}^{-1}\boldsymbol{C}^{(h)}\boldsymbol{N}\boldsymbol{E}_{2h}^{2m} = \sin\alpha\, \boldsymbol{E}_{hh}^{mm}$

Member's h characteristic stiffness matrix $\boldsymbol{k}_{AA}$ is then obtained:

$$\boldsymbol{k}_{AA} = \sum_{i=1}^{3}\sum_{j=1}^{3} EA\boldsymbol{l}^{-1}\boldsymbol{B}_{ih}\left(\boldsymbol{B}_{jh}\right)^{T}$$

$$\boldsymbol{k}_{AA} = \sum_{a=1}^{3}\sum_{b=1}^{3} \boldsymbol{E}_{ah}^{3m}\left(\left(\frac{\boldsymbol{\varepsilon} + \boldsymbol{I}^{mm}}{2}E_c - \frac{\boldsymbol{\varepsilon} - \boldsymbol{I}^{mm}}{2}E_b\right)\boldsymbol{A}\left(\boldsymbol{l}^{(0)}\right)^{-1}\boldsymbol{B}_{ah}\boldsymbol{B}_{bh}\right)\left(\boldsymbol{E}_{bh}^{3m}\right)^{T}$$

For truss and tensegrity structures respectively; E_b and E_c being the Young's modulus of the materials of which the bars and cables are made of.

The contribution of member h to the system stiffness matrix follows:

$$\underline{\underline{\boldsymbol{K}^{(h)}}} = \boldsymbol{G}^{(h)}\,\boldsymbol{k}_{AA}\left(\boldsymbol{G}^{(h)}\right)^{T}$$

Where $\boldsymbol{G}^{(h)}$ is of size $3p$ x 3 and has $-\boldsymbol{I}^{33}$ block at place $(1 \to 3, 3i-2 \to 3i)$ and a block $\boldsymbol{I}^{33}$ at place $(1 \to 3, 3j-2 \to 3j)$ such that $h = \zeta(\mathrm{i},\mathrm{j})$. $\boldsymbol{G}^{(h)}$ can also be derived from $\boldsymbol{C}^{(h)}$ with the following formula:

$$\boldsymbol{G}^{(h)} = \sum_{a=1}^{3} \boldsymbol{E}_{ah}^{3m}\boldsymbol{C}^{(h)}\left(\boldsymbol{E}_{h\,3(j-1)+a}^{m\,3p} - \boldsymbol{E}_{h\,3(i-1)+a}^{m\,3p}\right)$$

Finally, the system stiffness matrix $\underline{\underline{\boldsymbol{K}}}$ of size 3p x 3p (2p x 2p in 2D) such that $\underline{\boldsymbol{F}} = \underline{\underline{\boldsymbol{K}}}\,\underline{\boldsymbol{U}}$ where $\underline{\boldsymbol{F}}$ and $\underline{\boldsymbol{U}}$ are two vectors with respectively the components of the resulting forces applied and the displacements from the initial configuration to the deformed configuration of each node stacked all together is obtained by summing all the $\underline{\underline{\boldsymbol{K}^{(h)}}}$:

$$\underline{\underline{\boldsymbol{K}}} = \sum_{h=1}^{m} \underline{\underline{\boldsymbol{K}^{(h)}}}$$

A.1.3 Modification of the Static equilibrium equation to account for the supports

The static equilibrium equation being $\underline{f} = \underline{\underline{K}}\,\underline{U}$, in order for the system to be externally stable supports need to be provided. A certain number of degrees of freedom $\left(\underline{U}_{\sigma(i)}\right)_{i=1..s}$ are then set equal to zero and correspondingly if the resultant force vector $\underline{f}$ is decomposed into two parts, applied loads $\underline{Q}$ and reactions $\underline{R}$, only the components $\left(\underline{R}_{\sigma(i)}\right)_{i=1..s}$ are non-zero.

It exists a certain permutation of $[\![1,3p]\!]$ such that the first s components of $\left(\underline{U}_{\sigma(i)}\right)$ are all the supported degrees of freedom. The matrix of such a permutation is:

$$S_{ij} = \begin{cases} 1, & i = \sigma(j) \\ 0, & otherwise \end{cases}$$

Multiplying on the left by this matrix the equilibrium equation we get:

$$\begin{pmatrix} \boldsymbol{K_{FF}} & \boldsymbol{K_{FM}} \\ \boldsymbol{K_{MF}} & \boldsymbol{K_{MM}} \end{pmatrix} \begin{pmatrix} \mathbf{0} \\ \boldsymbol{U_M} \end{pmatrix} = \begin{pmatrix} \boldsymbol{Q_F} \\ \boldsymbol{Q_M} \end{pmatrix} + \begin{pmatrix} \boldsymbol{R_F} \\ \mathbf{0} \end{pmatrix}$$

Where $\boldsymbol{U_M} = \left(\underline{U}_{\sigma(i)}\right)_{i=s+1..3p}$, $\boldsymbol{Q_M} = \left(\underline{Q}_{\sigma(i)}\right)_{i=s+1..3p}$, $\boldsymbol{Q_F} = \left(\underline{Q}_{\sigma(i)}\right)_{i=1..s}$ and $\boldsymbol{R_F} = \left(\underline{R}_{\sigma(i)}\right)_{i=1..s}$.

Inversing the following linear system $\boldsymbol{K_{MM}}\boldsymbol{U_M} = \boldsymbol{Q_M}$, we get $\boldsymbol{U_M}$ and could potentially back-calculate the reactions.

The first output from this method is the displacement vector $\underline{U} = \boldsymbol{S}^{-1}\begin{pmatrix} \mathbf{0} \\ \boldsymbol{U_M} \end{pmatrix}$.

To get the forces in the members a few operations must be done. The coordinates of the nodes in the deformed configuration are:

$$\boldsymbol{N'} = \boldsymbol{N} + \sum_{i=1}^{3}\sum_{j=1}^{p} \boldsymbol{E}^{p\,3p}_{j\,(3j-3+i)}\,\underline{U}\boldsymbol{E}^{13}_{1i}$$

Subsequently, the length of the members in the deformed state is:

$$\boldsymbol{l'} = \sqrt{\sum_h (\boldsymbol{C}^{(h)}\boldsymbol{N'})(\boldsymbol{C}^{(h)}\boldsymbol{N'})^T}$$

The diagonal matrix with the elements' forces is then computed:

For a truss : $\boldsymbol{F} = E\boldsymbol{A}\boldsymbol{l}^{-1}(\boldsymbol{l'} - \boldsymbol{l})$

For a tensegrity : $\boldsymbol{F} = \left(\frac{\varepsilon+\boldsymbol{I}^{mm}}{2}E_c - \frac{\varepsilon-\boldsymbol{I}^{mm}}{2}E_b\right)\boldsymbol{A}\left(\boldsymbol{l}^{(0)}\right)^{-1}(\boldsymbol{l'} - \boldsymbol{l}) + \boldsymbol{F_0}$

Appendix 2 - Determinant calculation

Let n be a positive integer and $(\alpha_i, \beta_i)_{i=1..n} \in (\mathbb{R}^2)^n$. Consider the square matrix $\boldsymbol{Z^n}$ whose general term is:

$$(\boldsymbol{Z^n})_{ij} = \begin{cases} \alpha_j & for\ i \neq j \\ \alpha_j + \beta_j & for\ i = j \end{cases}$$

Show that:

$$|\boldsymbol{Z^n}| = \prod_{i=1}^{n} \beta_i + \sum_{i=1}^{n} \alpha_i \prod_{\substack{j=1 \\ j \neq i}}^{n} \beta_j$$

<u>Proof:</u> Subtracting the last row to all the rows before we get:

$$|\boldsymbol{Z^n}| = \begin{vmatrix} \beta_1 & 0 & \dots & 0 & -\beta_n \\ 0 & \beta_2 & \ddots & \vdots & -\beta_n \\ \vdots & \ddots & \ddots & 0 & \vdots \\ 0 & \dots & 0 & \beta_{n-1} & -\beta_n \\ \alpha_1 & \alpha_2 & \dots & \alpha_{n-1} & \alpha_n + \beta_n \end{vmatrix}$$

Developing from the last row:

$$|\boldsymbol{Z^n}| = \sum_{k=1}^{n-1} (-1)^{n+k} \alpha_k |\boldsymbol{Y_k}| + (\alpha_n + \beta_n) \prod_{k=1}^{n-1} \beta_k$$

Where $|\boldsymbol{Y_k}| = \begin{vmatrix} \boldsymbol{A_k} & \boldsymbol{B_k} \\ \boldsymbol{C_k} & \boldsymbol{D_k} \end{vmatrix}$, with

$$\boldsymbol{A_k} = \begin{pmatrix} \beta_1 & & \\ & \ddots & \\ & & \beta_{k-1} \end{pmatrix};\ \boldsymbol{B_k} = \begin{pmatrix} & & -\beta_n \\ & & \vdots \\ & & -\beta_n \end{pmatrix};\ \boldsymbol{C_k} = \boldsymbol{0}^{k-1,k-1};\ \boldsymbol{D_k} = \begin{pmatrix} 0 & & & -\beta_n \\ \beta_{k+1} & \ddots & & \vdots \\ & \ddots & 0 & \vdots \\ & & \beta_{n-1} & -\beta_n \end{pmatrix}$$

For $k = 1$ there is only $\boldsymbol{D_1}$ while for $k = n - 1$ there is only $\boldsymbol{A_{n-1}}$. The determinant of $\boldsymbol{Y_k}$ is then equal to $|\boldsymbol{Y_k}| = |\boldsymbol{A_k}||\boldsymbol{D_k}|$ for $k \neq 1, n - 1$ and $|\boldsymbol{Y_1}| = |\boldsymbol{D_1}|$, $|\boldsymbol{Y_{n-1}}| = |\boldsymbol{A_{n-1}}|$.

$|\boldsymbol{D_k}|$ is obtained by developing from the first row.

Finally,

$$|\boldsymbol{Z^n}| = \sum_{k=1}^{n-1} (-1)^{n+k} \alpha_k \left(\prod_{j=1}^{k-1} \beta_j \right) \left(-\beta_n (-1)^{n-k+1} \prod_{j=k+1}^{n-1} \beta_j \right) + (\alpha_n + \beta_n) \prod_{k=1}^{n-1} \beta_k$$

$$|\boldsymbol{Z^n}| = \prod_{i=1}^{n} \beta_i + \sum_{i=1}^{n} \alpha_i \prod_{\substack{j=1 \\ j \neq i}}^{n} \beta_j$$